NASA CR-165430

NASA-CR-165430
19840003447

A Reproduced Copy

OF

NASA CR-165,430

Reproduced for NASA

by the

NASA Scientific and Technical Information Facility

LIBRARY COPY

MAR 14 1984

LANGLEY RESEARCH CENTER
LIBRARY, NASA
HAMPTON, VIRGINIA

NF01557

FFNo 672 Aug 65

NASA CR-165430
BAT Report #D2536-941003

FINITE ELEMENT FORCED VIBRATION ANALYSIS OF ROTATING CYCLIC STRUCTURES

by

V. ELCHURI

G. C. C. SMITH

BELL AEROSPACE TEXTRON
P. O. Box One
Buffalo, New York 14240

NOV 1983
RECEIVED
NASA STI FACILITY
ACQ BRANCH

NATIONAL AERONAUTICS AND SPACE ADMINISTRATION

Contract NAS3-22533

NASA Lewis Research Center
Cleveland, Ohio 44135

NOV 1983
RECEIVED
NASA STI FACILITY
ACQ BRANCH

December 1981

(NASA-CR-165430) FINITE ELEMENT FORCED VIBRATION ANALYSIS OF ROTATING CYCLIC STRUCTURES Final Technical Report (Textron Bell Aerospace Co., Buffalo, N. Y.) 73 p HC A04/MF A01 CSCL 20K G3/39 N84-11515 Unclas 44557

N84-11515

1. Report No.	2. Government Accession No.	3. Recipient's Catalog No.
NASA CR-165430		

4. Title and Subtitle	5. Report Date
Finite Element Forced Vibration Analysis of Rotating Cyclic Structures	December 1981
	6. Performing Organization Code
7. Author(s)	8. Performing Organization Report No.
V. Elchuri, G. C. C. Smith	D2536-941008
	10. Work Unit No.
9. Performing Organization Name and Address	
Bell Aerospace Textron P. O. Box One Buffalo, New York 14240	11. Contract or Grant No. NAS3-22533
	13. Type of Report and Period Covered
12. Sponsoring Agency Name and Address	Contractor Report
NASA Lewis Research Center 21000 Brookpark Rd. Cleveland, Ohio 44135	14. Sponsoring Agency Code

15. Supplementary Notes

Richard E. Morris - Technical Monitor

Final Technical Report

16. Abstract

A new capability has been added to the general purpose finite element program NASTRAN Level 17.7 to conduct forced vibration analysis of tuned cyclic structures rotating about their axis of symmetry. The effects of Coriolis and centripetal accelerations together with those due to linear acceleration of the axis of rotation have been included.

This report presents the theoretical development of this new capability. The work was conducted under Contract NAS3-22533 from NASA Lewis Research Center, Cleveland, Ohio, with Mr. Richard E. Morris as the Technical Monitor.

17. Key Words (Suggested by Author(s))	18. Distribution Statement
Forced Vibrations, Rotating Cyclic Structures, NASTRAN, Finite Elements, Turbomachines, Propellers, Base Excitation	Publicly available

19. Security Classif. (of this report)	20. Security Classif. (of this page)	21. No. of Pages	22. Price*
Unclassified	Unclassified	71	

*For sale by the National Technical Information Service, Springfield, Virginia 22161

NASA-C-168 (Rev. 10-75)

NASA CR-165430
BAT Report #D2536-941008

FINITE ELEMENT FORCED VIBRATION ANALYSIS OF ROTATING CYCLIC STRUCTURES

by

V. ELCHURI

G. C. C. SMITH

BELL AEROSPACE TEXTRON
P. O. Box One
Buffalo, New York 14240

NATIONAL AERONAUTICS AND SPACE ADMINISTRATION

Contract NAS3-22533

NASA Lewis Research Center
Cleveland, Ohio 44135

December 1981

ABSTRACT

A new capability has been added to the general purpose finite element program NASTRAN Level 17.7 to conduct forced vibration analysis of tuned cyclic structures rotating about their axis of symmetry. The effects of Coriolis and centripetal accelerations together with those due to linear acceleration of the axis of rotation have been included.

This report presents the theoretical development of this new capability. The work was conducted under Contract NAS3-22533 from NASA Lewis Research Center, Cleveland, Ohio, with Mr. Richard E. Morris as the Technical Monitor.

SUMMARY

The objective of the work described herein, was the development, documentation, demonstration and delivery of a computer program for the forced vibration analysis of rotating cyclic structures. Tuned bladed discs are an example of specific interest.

The scope was by definition to address:

- direct periodic loads moving with the rotating structure , specified in the frequency or time domain;
- translational acceleration of the rotating axis.

The capability is operational in the NASTRAN general purpose program at Level 17.7.

NASTRAN documentation is provided and example analysis results have been obtained.

Relationships to previous work are described and further developments are recommended.

ACKNOWLEDGEMENT

The authors take this opportunity to express their deep appreciation of the programming efforts of Mr. A. Michael Gallo, Mr. Steven C. Skalski and Ms. Beverly J. Dale in implementing this theoretical development in NASTRAN. This report was typed by Mrs. Deanna L. Kutis.

TABLE OF CONTENTS

Section	Title	Page
	Abstract	ii
	Summary	iii
	Acknowledgement	iv
	List of Tables	vi
	List of Illustrations	vii
1	Introduction	1
2	Equations of Motion	5
3	Solution of Equations of Motion	15
4	Examples	25
5	Conclusions	57
6	Recommendations	58
	Appendix	59
	Symbols	62
	References	64

LIST OF TABLES

Table	Title	Page
1	Principal Features Demonstrated by Example Problems	28
2	Bladed Disc Natural Frequencies	29
3	Effect of Coriolis and Centripetal Accelerations on the Displacement Response of Grid Point 18 at 600 RPS	52
4	Comparison of Response at 1814 Hz.	55

LIST OF ILLUSTRATIONS

Figure	Title	Page
1	Main Problem Spectrum	2
2	Overall Program Structure and Status	3
3	Coordinate Systems	6
4	Overall Flowchart of Forced Vibration Analysis of Rotating Cyclic Structures	17,18
5	Directly Applied Periodic Loads Specified as Functions of Time	19
6	NASTRAN Model of the 12-Bladed Disc	26
7	NASTRAN Cyclic Model of the 12-Bladed Disc	27
8	k=2 Modes of Bladed Disc	30
9	Bladed Disc Example 1, Displacement Response (Magnitude)	32
10	Bladed Disc Example 1, Stress Response (Magnitude)	33
11	Bladed Disc Example 1, Stress Response (Magnitude)	34
12	Bladed Disc Example 2, Displacement Response (Magnitude)	36
13	Bladed Disc Example 2, Displacement Response (Magnitude)	37
14	Bladed Disc Example 2, Stress Response (Magnitude)	38
15	Bladed Disc Example 2, Stress Response (Magnitude)	39
16	Base Acceleration Data in an Inertial Coordinate System	42
17	Bladed Disc Example 3, Displacement Response (Magnitude)	43
18	Bladed Disc Example 3, Stress Response (Magnitude)	44
19	Bladed Disc Example 3, Displacement Response (Magnitude)	45
20	Bladed Disc Example 3, Stress Response (Magnitude)	46
21	Bladed Disc Example 3, Displacement Response (Phase)	47
22	Bladed Disc Example 3, Displacement Response (Magnitude)	48
23	Bladed Disc Example 3, Stress Response (Magnitude)	49
24	Bladed Disc Example 3, Displacement Response (Magnitude)	50
25	Bladed Disc Example 3, Stress Response (Magnitude)	51

1. INTRODUCTION

In Reference 1 (NASA CR159728), a general approach to conducting dynamics analysis of bladed discs was discussed and a logical sequence of problems defined. Figure 1 indicates the problem spectrum and Figure 2 shows an overall program structure of modular nature, based on additions and modifications to the NASTRAN general purpose structural analysis program.

The general set of problems can be represented by formal equations, various terms of which are included or excluded depending on the problem being studied. Thus the equations

$$[M]\{\ddot{u}\} + [[B] + 2\Omega[B_1]]\{\dot{u}\} - [Q]\{u\} + [[K] - \Omega^2[M_1]]\{u\} = \{P\} - [M_2]\{\ddot{R}_o\}, \qquad (1)$$

with some boundary conditions, may be taken to represent the general forced vibration dynamic problem of a tuned bladed disc. In the previous and current work, the advantages of cyclic symmetry are incorporated in this formulation.

The work of Reference 1 handled, within state-of-the-art technology, analyses of aeroelastic, modal and flutter problems of tuned cyclic structures (Figure 2). It was documented and operated in NASTRAN at Levels 16 (Refs. 2 - 5), and 17.7 (Ref. 6).

The equations

$$[M]\{\ddot{u}\} + [B]\{\dot{u}\} - [Q]\{u\} + [K]\{u\} = \{0\} \qquad (2)$$

were treated in the context of modal and flutter problems of a tuned system, where

M represented the inertia matrix;
B represented the damping matrix;
Q represented the induced aerodynamic matrix (complex);
and K represented the elastic cum geometric stiffness matrix.

In the current work, the equations

$$[M]\{\ddot{u}\} + [[B] + 2\Omega[B_1]]\{\dot{u}\} + [[K] - \Omega^2[M_1]]\{u\} = \{P\} - [M_2]\{\ddot{R}_o\} \qquad (3)$$

are treated in the context of forced vibration, (Figure 2),

ORIGINAL PAGE IS
OF POOR QUALITY

Aerothermoelastic Problems
(Constant Speed)

A.1	"As Manufactured" Shape at the Design Point	*
A.2	Off-Design Point Performance Analysis	*
A.3	Transient Aerothermoelastic Performance	Δ

Elastic and geometric (differential) stiffness effects.

Tuned System Dynamics
(Constant Speed, Pressure Ratio and Flow Rate)

T.1	In-Vacuo Modal Analysis	*
T.2	"Running" Modal Analysis	*
T.3	Flutter Boundaries	*
T.4	Sub-critical Eigenvalues	*
T.5	Forced Vibration Response	*

Basis for Perturbation and Fourier Expansion Techniques

Mistuned Systems Dynamics
(Constant Speed, Pressure Ratio and Flow Rate)

M.1	In Vacuo Modal Analysis	O
M.2	"Running" Modal Analysis	O
M.3	Flutter Boundaries	O
M.4	Sub-critical Eigenvalues	O
M.5	Forced Vibration Response	O

NOTES:

1. After design point A.1, A.2 gives the elastic system "Map" within aerodynamic program limitations
2. T.1, T.2, are functions of selected operating points on the Compressor Map.
3. T.3 uses modes from T.2.
4. T.4 uses harmonic aerodynamics from T.3.
5. T.5 uses complex eigenvalues from T.4.
6. M.1, M.2 use the modal information from T.1, T.2,
7. M.3, M.4 use T.3 harmonic aerodynamics and Fourier expansion techniques. (Cascade theories limit validity)
8. M.5 uses complex eigenvalues from M.4.
9. * - Operational
   O - Methods Formulated
   Δ - Approach Conceptualized.

Figure 1: Main Problem Spectrum

ORIGINAL PAGE IS
OF POOR QUALITY

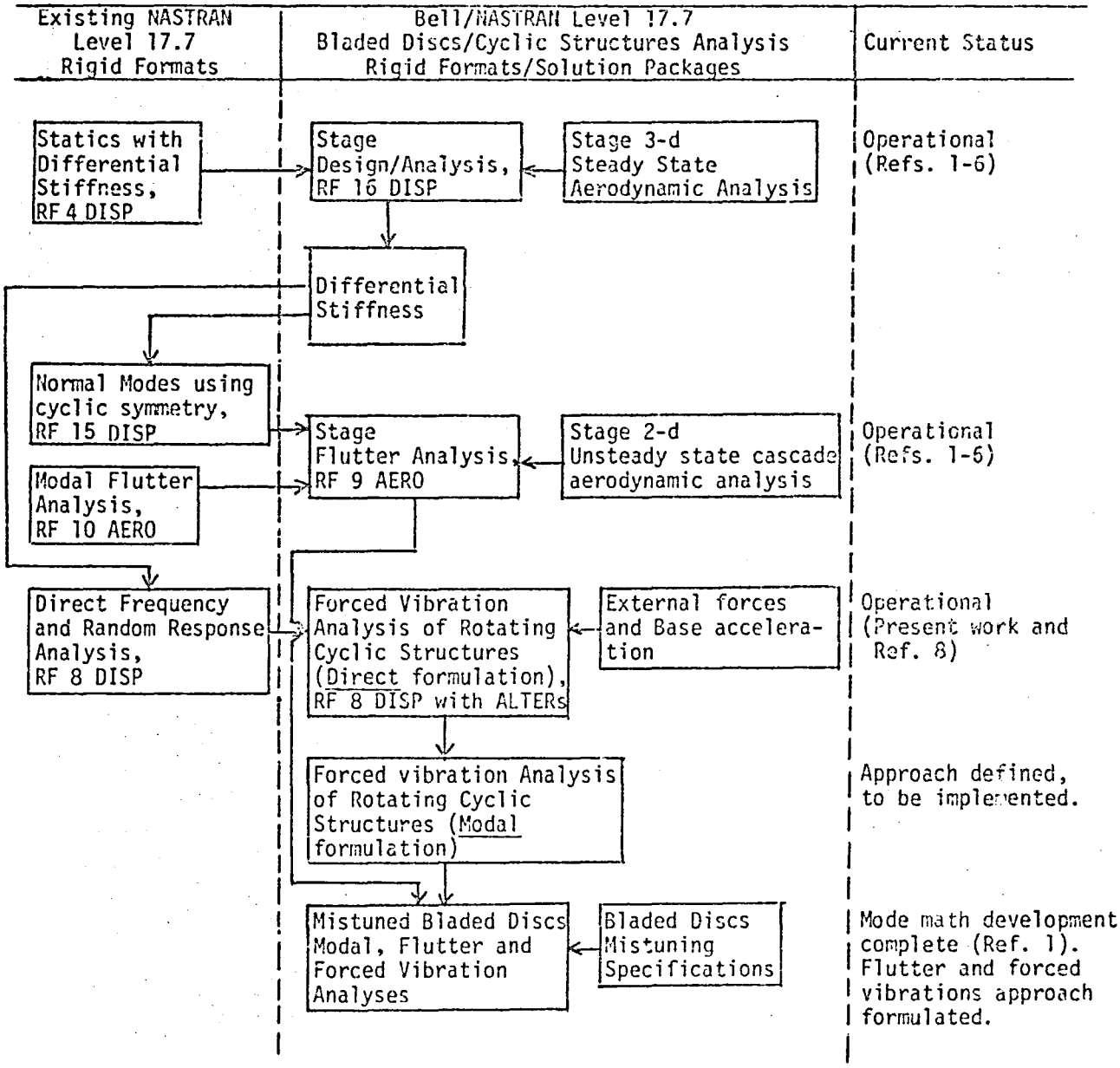

Figure 2: Overall Program Structure & Status

where [M], [B], [K] are as before,

$[B_1]$ represents Coriolis forces matrix

$\{P\}$ represents applied surface load vector

$[M_2]$ represents base forcing mass matrix

and $\{\ddot{R}_0\}$ represents base acceleration vector.

The specific form of the forced vibration equations including the types of forcing functions to be incorporated were selected by NASA. These are specifically

- directly applied loads moving with the rotating structure;
- inertial loads due to translational accelerations of the axis of rotation ("base acceleration").

The loads may be periodic and specified in the frequency or time domains. Solution procedures follow generally those of the cyclic symmetry formulation of the NASTRAN Theoretical Manual (Ref. 7). The capability has been developed on the IBM 370 system at Bell Aerospace Textron and documented, delivered and demonstrated on the UNIVAC 1108 at NASA Lewis in NASTRAN Level 17.7.

Five demonstration examples are presented, one being a complete structure example to show compatibility with the cyclic structure formulation. A simple twelve bladed disc is modelled and forced at conditions related to its natural frequencies. The response examples include:

- physical component forcing (frequency domain),
- harmonic component forcing (frequency domain),
- harmonic component forcing of the rotational axis,
- physical periodic forcing (time domain),
- harmonic component periodic forcing (time domain)

It would be logical to extend the current work to include the generation of applied and induced oscillatory aerodynamic loads so that the forced vibrations of subcritical engine stages can be addressed directly. Rotational base accelerations could also be of practical interest in investigating the gyroscopic effects on rotating machinery.

2. EQUATIONS OF MOTION

The equations of motion of a tuned cyclic structure rotating about its axis of symmetry and subjected to steady sinusoidal and general periodic excitation are derived using Lagrange's formulation.

Figure 3 illustrates the problem by considering a 12-bladed disc as an example. The bladed disc consists of twelve 30° segments--identical in their geometric, material and constraint properties. The disc rotates about its axis of symmetry at a constant angular velocity. The axis of rotation itself is permitted to oscillate linearly in any given inertial reference. In addition, the bladed disc is allowed to be loaded with steady sinusoidal or general periodic loads moving with the structure. Under these conditions, it is desired to determine the dynamic response (displacement, acceleration, stress, etc.) of the bladed disc.

The cyclic symmetry feature of the rotating structure is utilized in deriving and solving the equations of forced motion. Consequently, only one of the cyclic sectors is modelled and analyzed using finite elements, yielding substantial savings in the analysis cost. Results, however, are obtained for the entire structure. The Coriolis and centripetal acceleration terms have been included. For clarity of derivation, the equations of motion are first derived for an arbitrary grid point of the cyclic sector finite element model, and then extended for the complete model.

COORDINATE SYSTEMS

These are shown in Figure 3. O-XYZ is an inertial coordinate system. $O\text{-}X_BY_BZ_B$ is a body-fixed coordinate system such that OX_B coincides with the axis of rotation of the structure and is always parallel to OX. For a NASTRAN finite element model of the bladed disc, $O\text{-}X_BY_BZ_B$ also represents the Basic coordinate system. A-xyz is a body-fixed global coordinate system in which the displacements of any grid point P are desired. The unit vectors associated with these coordinate systems are also shown in Figure 3 .

DEGREES OF FREEDOM

The rotating structure is permitted four rigid body motions including three translations (along OX, OY and OZ) and one rotation at a constant angular velocity Ω about its axis of rotation OX_B.

ORIGINAL PAGE IS
OF POOR QUALITY

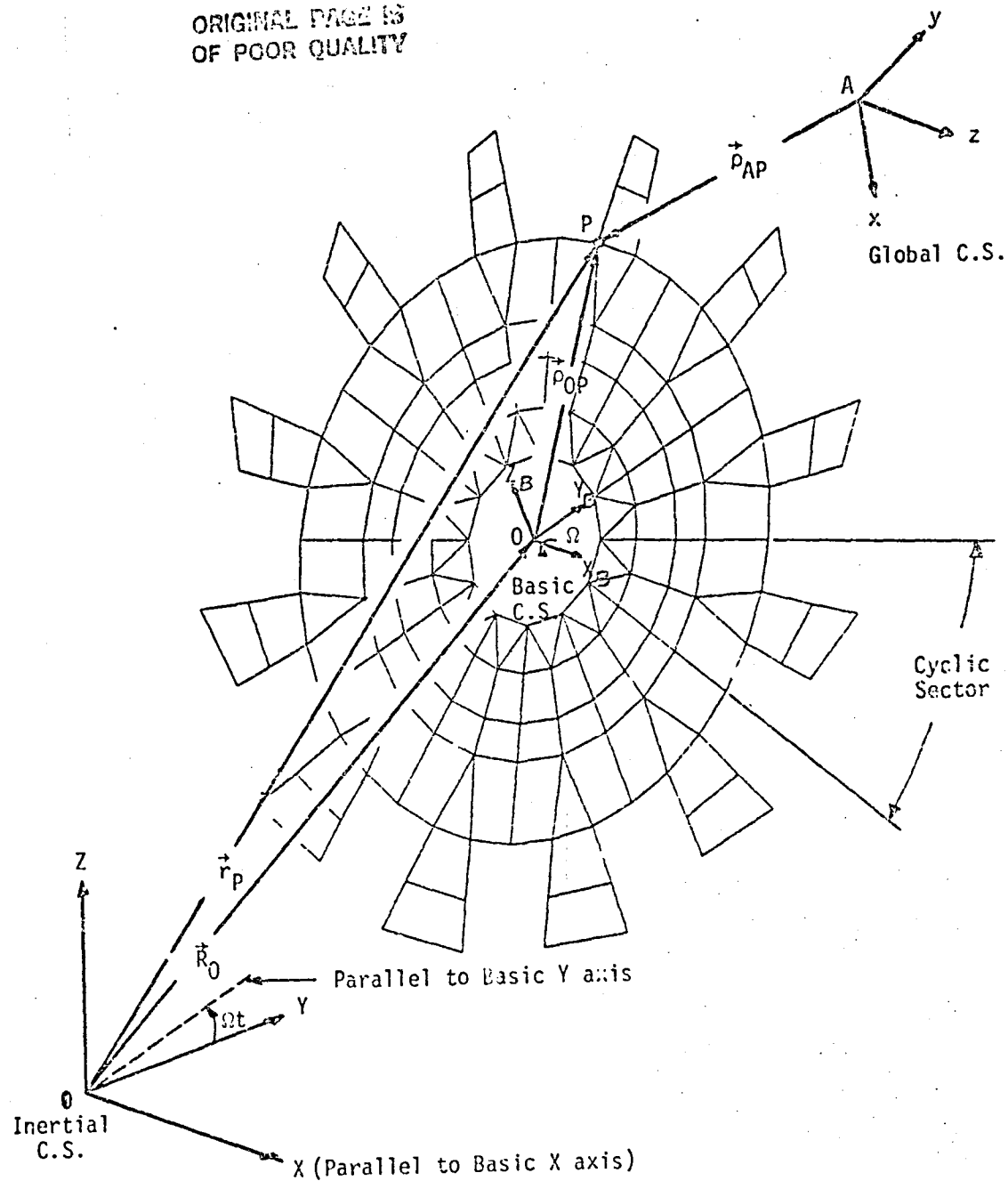

$\hat{I}, \hat{J}, \hat{K}$ Unit vectors along Inertial XYZ axes

$\hat{I}_B, \hat{J}_B, \hat{K}_B$ Unit vectors along Basic $X_BY_BZ_B$ axes

$\hat{i}, \hat{j}, \hat{k}$ Unit vectors along Global xyz axes

Figure 3: Coordinate Systems

ORIGINAL PAGE IS
OF POOR QUALITY

All grid points of the structure are each permitted six degrees of freedom. The displacement at any grid point in any sector can be expressed in any body-fixed coordinate system as a combination of:

1) the steady state displacement due to the steady rotation of, and the steady state loads applied to, the structure, and

2) the vibratory displacement (superposed on the steady displacement) due to the vibratory excitation provided by the directly applied loads and the inertial loads due to the acceleration of the axis of rotation ('base' acceleration).

The purpose of the present development is to determine the vibratory response.

LAGRANGE FORMULATION

Referring to Figure 3, the complete tuned structure consists of N identical cyclic sectors. If u represents all the vibratory degrees of freedom of the complete structure, the equations of motion can be derived via the Lagrange formulation,

$$\frac{d}{dt}\left(\frac{\partial T}{\partial \dot{u}}\right) - \frac{\partial T}{\partial u} + \frac{\partial U}{\partial u} + \frac{\partial D}{\partial \dot{u}} = \frac{\partial W}{\partial u} \quad , \tag{1}$$

where T and U represent the kinetic and strain energies, respectively, of the complete structure; D is the Rayleigh's dissipation function representing the energy lost in the system due to resisting forces proportional to velocities $\dot{u}$ (e.g. viscous damping forces); and δW represents the virtual work done on the structure by the external forces through virtual displacements δu.

The complete set of degrees of freedom u can be subdivided into N subsets, each containing u^n degrees of freedom for each of the N cyclic sectors. Since any given cyclic sector is 'connected' to adjacent cyclic sectors only on its two sides, u^n satisfies the intersector boundary compatibility condition

$$u^n_{\text{side 2}} = u^{n+1}_{\text{side 1}} \quad , \quad n = 1, 2, \ldots, N. \tag{2}$$

Equations (1), therefore, can be written as N sets of equations coupled only as given by equations (2):

$$\frac{d}{dt}\left(\frac{\partial T^n}{\partial \dot{u}^n}\right) - \frac{\partial T^n}{\partial u^n} + \frac{\partial U^n}{\partial u^n} + \frac{\partial D^n}{\partial \dot{u}^n} = \frac{\partial W^n}{\partial u^n} \, , \qquad n = 1, 2, \ldots, N \, . \tag{3}$$

ORIGINAL PAGE IS
OF POOR QUALITY

For clarity of presentation, without loss of generality, equations (3) are first applied to obtain the equations of motion of an arbitrary grid point in any cyclic sector by considering its three translational degrees of freedom. Inclusion of the three rotational degrees of freedom at the arbitrary grid point, and extension to include the remaining grid points in the cyclic sector are considered subsequently.

KINETIC ENERGY

With reference to Figure 3, point P is an arbitrary grid point of the nth cyclic sector with a mass of 'm' units lumped from the adjacent finite elements.

The kinetic energy of the mass at P can be written as:

$$T = \frac{1}{2} m \dot{\vec{r}}_P \cdot \dot{\vec{r}}_P \tag{4}$$

where

$$\dot{\vec{r}}_P = \dot{\vec{R}}_0 + \dot{\vec{\rho}}_{0P} + (\vec{\Omega} \times \vec{\rho}_{0P}), \tag{5}$$

$$\dot{\vec{R}}_0 = \dot{X}_0 \hat{I} + \dot{Y}_0 \hat{J} + \dot{Z}_0 \hat{K} \quad , \tag{6}$$

$$\dot{\vec{\rho}}_{0P} = \dot{X}_{0P} \hat{I}_B + \dot{Y}_{0P} \hat{J}_B + \dot{Z}_{0P} \hat{K}_B \ , \tag{7}$$

$$\vec{\Omega} = \Omega \hat{I} \quad , \tag{8}$$

and

$$\begin{Bmatrix} \hat{I}_B \\ \hat{J}_B \\ \hat{K}_B \end{Bmatrix} = \begin{bmatrix} 1 & 0 & 0 \\ 0 & c & s \\ 0 & -s & c \end{bmatrix} \begin{Bmatrix} \hat{I} \\ \hat{J} \\ \hat{K} \end{Bmatrix} \quad , \tag{9}$$

with $\quad c \equiv \cos \Omega t$ and $s \equiv \sin \Omega t \quad .$ (10)

Substitution of equations (5) through (9) in equation (4) results in

$$T = \frac{1}{2} \lfloor \dot{X}_0 \ \dot{Y}_0 \ \dot{Z}_0 \rfloor \begin{bmatrix} m & & \\ & m & \\ & & m \end{bmatrix} \begin{Bmatrix} \dot{X}_0 \\ \dot{Y}_0 \\ \dot{Z}_0 \end{Bmatrix}$$

$$+ \frac{1}{2} \lfloor \dot{X}_{0P} \ \dot{Y}_{0P} \ \dot{Z}_{0P} \rfloor \begin{bmatrix} m & & \\ & m & \\ & & m \end{bmatrix} \begin{Bmatrix} \dot{X}_{0P} \\ \dot{Y}_{0P} \\ \dot{Z}_{0P} \end{Bmatrix}$$

ORIGINAL PAGE IS
OF POOR QUALITY

$$+ \frac{1}{2}\ \Omega^2 \ \lfloor X_{OP}\ Y_{OP}\ Z_{OP} \rfloor \begin{bmatrix} 0 & 0 & 0 \\ 0 & m & 0 \\ 0 & 0 & m \end{bmatrix} \begin{Bmatrix} X_{OP} \\ Y_{OP} \\ Z_{OP} \end{Bmatrix}$$

$$+ \ \lfloor \mathring{X}_{OP}\ \mathring{Y}_{OP}\ \mathring{Z}_{OP} \rfloor \begin{bmatrix} m & 0 & 0 \\ 0 & mc & ms \\ 0 & -ms & mc \end{bmatrix} \begin{Bmatrix} \mathring{X}_0 \\ \mathring{Y}_0 \\ \mathring{Z}_0 \end{Bmatrix}$$

$$+ \Omega \ \lfloor \mathring{X}_{OP}\ \mathring{Y}_{OP}\ \mathring{Z}_{OP} \rfloor \begin{bmatrix} 0 & 0 & 0 \\ 0 & 0 & -m \\ 0 & m & 0 \end{bmatrix} \begin{Bmatrix} X_{OP} \\ Y_{OP} \\ Z_{OP} \end{Bmatrix}$$

$$+ \Omega \ \lfloor X_{OP}\ Y_{OP}\ Z_{OP} \rfloor \begin{bmatrix} 0 & 0 & 0 \\ 0 & -ms & mc \\ 0 & -mc & -ms \end{bmatrix} \begin{Bmatrix} \mathring{X}_0 \\ \mathring{Y}_0 \\ \mathring{Z}_0 \end{Bmatrix} . \tag{11}$$

In order to introduce the global coordinates of point P, consider now the position vector to P written as

$$\overrightarrow{OP} = \overrightarrow{OA} + \overrightarrow{AP} \quad , \tag{12}$$

i.e.

$$\lfloor X_{OP}\ Y_{OP}\ Z_{OP} \rfloor \begin{Bmatrix} \hat{I}_B \\ \hat{J}_B \\ \hat{K}_B \end{Bmatrix} = \lfloor X_{OA}\ Y_{OA}\ Z_{OA} \rfloor \begin{Bmatrix} \hat{I}_B \\ \hat{J}_B \\ \hat{K}_B \end{Bmatrix} + \lfloor x_{AP}\ y_{AP}\ z_{AP} \rfloor \begin{Bmatrix} \hat{i} \\ \hat{j} \\ \hat{k} \end{Bmatrix} , \tag{13}$$

where

$$\begin{Bmatrix} \hat{i} \\ \hat{j} \\ \hat{k} \end{Bmatrix} = \left[T^{\text{Basic to Global}} \right] \begin{Bmatrix} \hat{I}_B \\ \hat{J}_B \\ \hat{K}_B \end{Bmatrix} . \tag{14}$$

ORIGINAL PAGE IS
OF POOR QUALITY

Therefore equation (13) yields

$$\begin{Bmatrix} X_{OP} \\ Y_{OP} \\ Z_{OP} \end{Bmatrix} = \begin{Bmatrix} X_{OA} \\ Y_{OA} \\ Z_{OA} \end{Bmatrix} + [T^{GB}] \begin{Bmatrix} x_{AP} \\ y_{AP} \\ z_{AP} \end{Bmatrix} , \tag{15}$$

noting that $[T^{GB}] = [T^{BG}]^T$. (16)

The global position vector to the point P can be further thought of as consisting of three component vectors, i.e.,

$$\begin{Bmatrix} x_{AP} \\ y_{AP} \\ z_{AP} \end{Bmatrix} = \underbrace{\underbrace{\begin{Bmatrix} x_{AP} \\ y_{AP} \\ z_{AP} \end{Bmatrix}_{\text{initial}}}_{\text{Initial position}} + \underbrace{\begin{Bmatrix} \bar{u}_x \\ \bar{u}_y \\ \bar{u}_z \end{Bmatrix}}_{\text{Displacements due to } \Omega \text{ and steady loads}}}_{\text{Steady part}} + \underbrace{\underbrace{\begin{Bmatrix} u_x \\ u_y \\ u_z \end{Bmatrix}}_{\text{Displacements due to vibratory forces}}}_{\text{Vibratory part}} . \tag{17}$$

Substitution of equations (17) in equations (15), and differentiation once with respect to t yields

$$\begin{Bmatrix} \dot{X}_{OP} \\ \dot{Y}_{OP} \\ \dot{Z}_{OP} \end{Bmatrix} = [T^{GB}] \begin{Bmatrix} \dot{u}_x \\ \dot{u}_y \\ \dot{u}_z \end{Bmatrix} . \tag{18}$$

Therefore, with the help of equations (15), (17) and (18), equation (11) expresses the kinetic energy of the mass at P in terms of the displacements and velocities of P expressed in the global coordinate system A-xyz.

STRAIN ENERGY

The strain energy due to the displacements at point P expressed in the basic coordinate system can be written as

$$U = \frac{1}{2} \left\lfloor (X_{OP} - X_{OP,\,in.}) , (Y_{OP} - Y_{OP,\,in.}) , (Z_{OP} - Z_{OP,\,in.}) \right\rfloor * \begin{bmatrix} K_{XX} & K_{XY} & K_{XZ} \\ K_{YX} & K_{YY} & K_{YZ} \\ K_{ZX} & K_{ZY} & K_{ZZ} \end{bmatrix} * \begin{Bmatrix} X_{OP} - X_{OP,in.} \\ Y_{OP} - Y_{OP,in.} \\ Z_{OP} - Z_{OP,in.} \end{Bmatrix} . \tag{19}$$

ORIGINAL PAGE IS
OF POOR QUALITY

By using equations (15) and (17), this becomes

$$U = \frac{1}{2} \lfloor (\bar{u}_x + u_x), (\bar{u}_y + u_y), (\bar{u}_z + u_z) \rfloor [K^{Global}] \begin{Bmatrix} \bar{u}_x + u_x \\ \bar{u}_y + u_y \\ \bar{u}_z + u_z \end{Bmatrix} , \tag{20}$$

where $$[K^{Global}] = [T^{GB}]^T [K^{Basic}] [T^{GB}] \quad . \tag{21}$$

DISSIPATED ENERGY

The energy dissipated by the damping forces acting against the motion of the point P is expressed by the Rayleigh's dissipation function,

$$D = \frac{1}{2} \lfloor \mathring{X}_{OP} \quad \mathring{Y}_{OP} \quad \mathring{Z}_{OP} \rfloor \begin{bmatrix} B_{XX} & B_{XY} & B_{XZ} \\ B_{YX} & B_{YY} & B_{YZ} \\ B_{ZX} & B_{ZY} & B_{ZZ} \end{bmatrix}^{Basic} \begin{Bmatrix} \mathring{X}_{OP} \\ \mathring{Y}_{OP} \\ \mathring{Z}_{OP} \end{Bmatrix} . \tag{22}$$

Use of equation (18) transforms this to

$$D = \frac{1}{2} \lfloor \mathring{u}_x \quad \mathring{u}_y \quad \mathring{u}_z \rfloor [B^{Global}] \begin{Bmatrix} \mathring{u}_x \\ \mathring{u}_y \\ \mathring{u}_z \end{Bmatrix} , \tag{23}$$

where $$[B^{Global}] = [T^{GB}]^T [B^{Basic}] [T^{GB}] \quad . \tag{24}$$

VIRTUAL WORK

The virtual work done by an oscillatory applied load

$$\vec{P} = P_x \hat{i} + P_y \hat{j} + P_z \hat{k} \quad , \tag{25}$$

moving with the point of application, through individually achieved virtual displacements δu_x, δu_y and δu_z can be stated as

$$\delta W = \delta \lfloor u_x \; u_y \; u_z \rfloor \begin{Bmatrix} P_x \\ P_y \\ P_z \end{Bmatrix} . \tag{26}$$

ORIGINAL PAGE IS
OF POOR QUALITY

EQUATIONS OF FORCED MOTION

Substitution of the expressions for T (equation 11), U (equation 20), D (equation 23) and δW (equation 26) in the Lagrange equations (3) results in the following equations of forced motion of point P expressed in the displacement (global) coordinate system A-xyz:

$$[M]\{\ddot{u}\} + \Big[[B] + 2\Omega[B_1]\Big]\{\dot{u}\} + \Big[[K] - \Omega^2[M_1]\Big]\{u\} = \{P\} - [M_2]\{\ddot{R}_0\} . \tag{27}$$

The terms appearing in equations (27) are:

$$\{u\} = \begin{Bmatrix} u_x \\ u_y \\ u_z \end{Bmatrix} , \tag{28}$$

$$\{P\} = \begin{Bmatrix} P_x \\ P_y \\ P_z \end{Bmatrix} , \tag{29}$$

$$\{\ddot{R}_0\} = \begin{Bmatrix} \ddot{X}_0 \\ \ddot{Y}_0 \\ \ddot{Z}_0 \end{Bmatrix} , \tag{30}$$

$$[M] = [M]^{global} = [T^{GB}]^T \begin{bmatrix} m & 0 & 0 \\ 0 & m & 0 \\ 0 & 0 & m \end{bmatrix} [T^{GB}] , \tag{31}$$

$$[B] = [B]^{global} \tag{24}$$

$$[B_1] = [B_1]^{global} = [T^{GB}]^T \begin{bmatrix} 0 & 0 & 0 \\ 0 & 0 & -m \\ 0 & m & 0 \end{bmatrix} [T^{GB}] , \tag{32}$$

$$[K] = [K]^{global} \tag{21}$$

$$[M_1] = [M_1]^{global} = [T^{GB}]^T \begin{bmatrix} 0 & 0 & 0 \\ 0 & m & 0 \\ 0 & 0 & m \end{bmatrix} [T^{GB}] , \tag{33}$$

and

$$[M_2] = [T^{GB}]^T \begin{bmatrix} m & 0 & 0 \\ 0 & mc & ms \\ 0 & -ms & mc \end{bmatrix} , \tag{34}$$

where c and s are given by equation (10).

Equations(27) describe the translatory motion of an arbitrary point P in an arbitrary sector n of the rotating cyclic structure subjected to a directly applied vibratory load {P} and base acceleration $\{\ddot{R}_0\}$.

These equations can be extended to include the three rotational degrees of freedom at point P by noting that:

1) in a lumped mass model, only the translational degrees of freedom at any grid point contribute to the kinetic energy of the structure, and

2) the coupling between various degrees of freedom may exist only via the stiffness matrix. (Instances where the damping matrix is defined proportional to the stiffness matrix also may result in coupled equations of motion.)

Accordingly, the matrices derived from kinetic energy considerations, viz. $[M]$, $[B_1]$, $[M_1]$ and $[M_2]$ of equation (27) can be expanded as typified by

$$\underset{6x6}{[M]} = \left[\begin{array}{c|c} [M_{tt}] & 0 \\ \hline 0 & 0 \end{array}\right] , \tag{35}$$

where $[M_{tt}]$ is the 3x3 (translational) mass matrix of equation (27). With subscripts t and r representing the translational and rotational degrees of freedom at point P, the stiffness and damping matrices may be expanded as

$$[K] = \left[\begin{array}{c|c} [K_{tt}] & [K_{tr}] \\ \hline [K_{rt}] & [K_{rr}] \end{array}\right] , \tag{36}$$

and

$$[B] = \left[\begin{array}{c|c} [B_{tt}] & [B_{tr}] \\ \hline [B_{rt}] & [B_{rr}] \end{array}\right] . \tag{37}$$

By similar reasoning, the equations of forced vibratory motion of all the cyclic sectors of the total structure can be written as

$$[M^n]\{\ddot{u}^n\} + \left[[B^n] + 2\Omega[B_1^n]\right]\{\dot{u}^n\} + \left[[K^n] - \Omega^2[M_1^n]\right]\{u^n\} = \{P^n\} - [M_2^n]\{\ddot{R}_0\},$$

$$n = 1, 2, \ldots, N. \quad (38)$$

The intersegment boundary compatibility is specified by equation (2).

3. SOLUTION OF EQUATIONS OF MOTION

The method of solution of the equations of forced motion (equations 38 and 2, Section 2) is based upon the form in which the excitation of the rotating structure is specified. As noted earlier, the present development considers excitation prescribed as:

1) directly applied loads moving with the structure and

2) inertial loads due to the translational acceleration of the axis of rotation ('base' acceleration).

These steady-state sinusoidal or general periodic loads are specified to represent:

1) the physical loads on various segments of the complete structure, or

2) the circumferential harmonic components of the loads in (1).

The sinusoidal loads are specified as functions of frequency and the general periodic loads are specified as functions of time.

The translational acceleration of the axis of rotation is specified as a function of frequency in an inertial coordinate system.

Because of its eventual implementation in the NASTRAN general purpose finite element structural analysis program, the following solution procedure generally follows the theoretical presentation of cyclic symmetry given in the NASTRAN Theoretical Manual (Ref. 7).

METHOD OF SOLUTION

The method of solution of the equations of motion consists of four principal steps:

1) Transformation of applied loads to frequency-dependent circumferential harmonic components.

2) Application of circumferential harmonic-dependent inter-segment compatibility constraints.

3) Solution of frequency-dependent circumferential harmonic components of displacements.

4) Recovery of frequency-dependent response (displacements, stresses, loads, etc.) in various segments of the total structure.

An overall flowchart outlining the solution algorithm is shown in Figure 4. Provision to include the differential stiffness due to the steady loads is also shown.

1. Transformation of Applied Loads

The transformation to frequency-dependent circumferential harmonic components depends on the form in which the excitation is specified by the user. The following options are considered in the present development to specify the form of excitation due to the directly applied loads and base acceleration loads:

Directly applied loads specified as:

- periodic functions of time on various segments,
- periodic functions of time for various circumferential harmonic indices
- functions of frequency on various segments
- functions of frequency for various circumferential harmonic indices.

Base acceleration specified as:

- function of frequency for circumferential harmonic indices 0 (axial) and 1 (lateral).

Details of each of the above five loading conditions are as follows:

Directly applied loads (segment-dependent and periodic in time)

If P^n represents a general periodic load on sector n specified as a function of time at M equally spaced instances of time per period (Figure 5), the load at m^{th} time instant can be written as

$$\overset{m}{P}{}^n = \overset{-o}{P}{}^n + \sum_{\ell=1}^{\ell_L} \left[\overset{-\ell c}{P}{}^n \cos(\overline{m-1}\ell b) + \overset{-\ell s}{P}{}^n \sin(\overline{m-1}\ell b) \right] + (-1)^{m-1} \overset{-M/2}{P}{}^n \quad , \qquad (1)$$

$$m = 1, 2, \ldots, M \quad ,$$

where $b = 2\pi/M$, $\ell_L = (M-1)/2$ for odd M, $\ell_L = (M-2)/2$ for even M. The last term in equation (1) exists only when M is even. The coefficients $\overset{-}{P}{}^{n}{}^{\ell}$ ("ℓ" = 0; ℓc, ℓs, ℓ=1, 2, ..., ℓ_L; M/2) in equation (1) are independent of time, and are defined by the relations

$$\overset{-o}{P}{}^n = \frac{1}{M} \sum_{m=1}^{M} \overset{m}{P}{}^n \quad , \qquad (\ell = 0) \qquad \text{Part of (2)}$$

ORIGINAL PAGE IS
OF POOR QUALITY

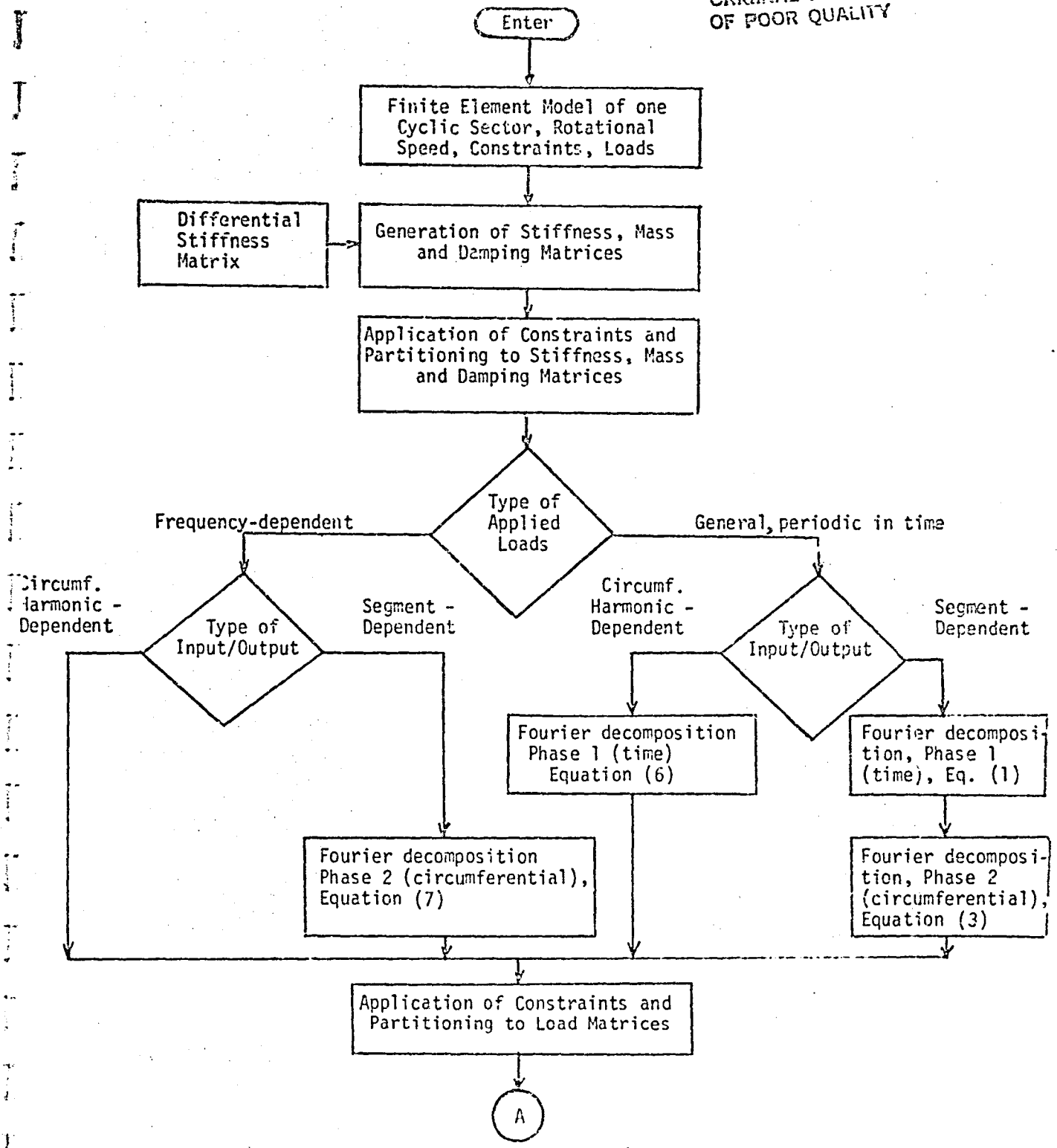

FIGURE 4: Overall Flowchart of Forced Vibration Analysis of Rotating Cyclic Structures

ORIGINAL PAGE IS
OF POOR QUALITY

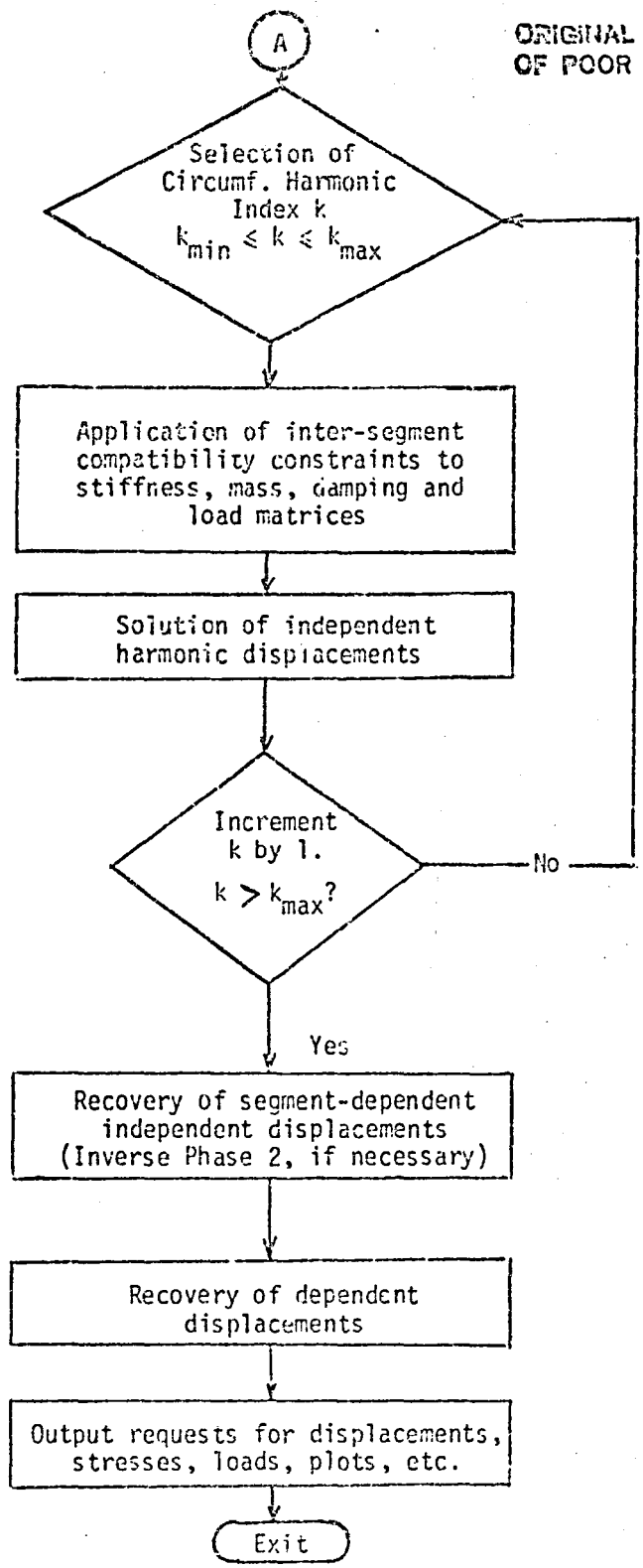

FIGURE 4. (Concluded)

ORIGINAL PAGE IS
OF POOR QUALITY

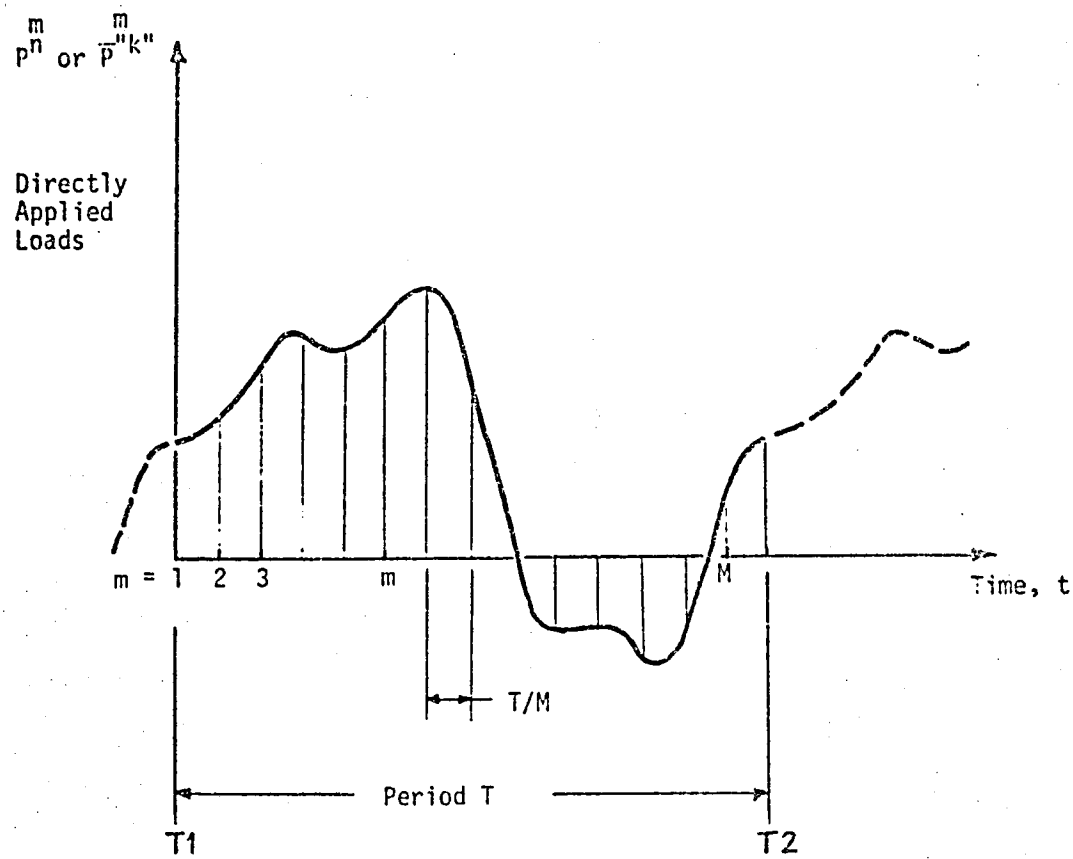

Figure 5: Directly Applied Periodic Loads Specified as Functions of Time

ORIGINAL PAGE IS
OF POOR QUALITY

$$\left.\begin{aligned}
&\left.\begin{aligned}
\bar{P}^{n\ell c} &= \frac{2}{M}\sum_{m=1}^{M} P^{m}_{n} \cos(\overline{m-1}\ell b), \\
\bar{P}^{n\ell s} &= \frac{2}{M}\sum_{m=1}^{M} P^{m}_{n} \sin(\overline{m-1}\ell b), \quad \text{and}
\end{aligned}\right\} (\ell=1, 2, \ldots, \ell_L) \\
&\bar{P}^{nM/2} = \frac{1}{M}\sum_{m=1}^{M} (-1)^{m-1} P^{m}_{n} \ (M \text{ even only}) \quad (\ell=M/2).
\end{aligned}\right\} \text{(2 Contd.)}$$

Each of the coefficient vectors $\bar{P}^{n\text{"}\ell\text{"}}$ on the left hand sides of equations (2) can further be expanded in a circumferential (truncated) Fourier series

$$\bar{P}^{n\text{"}\ell\text{"}} = \bar{P}^{0\text{"}\ell\text{"}} + \sum_{k=1}^{k_L} \left[\bar{P}^{k\text{"}\ell\text{"}c} \cos(\overline{n-1}ka) + \bar{P}^{k\text{"}\ell\text{"}s} \sin(\overline{n-1}ka)\right] + (-1)^{n-1}\bar{P}^{N/2\text{"}\ell\text{"}} , \tag{3}$$

$$\left.\begin{aligned}
&\text{where } n = 1, 2, \ldots, N , \\
&\text{"}\ell\text{"} = 0;\ \ell c,\ \ell s, \ell = 1, 2, \ldots, \ell_L;\ M/2 \\
&a = 2\pi/N \\
&k_L = (N-1)/2 \text{ for } N \text{ odd} \\
&k_L = (N-2)/2 \text{ for } N \text{ even.}
\end{aligned}\right\} \tag{4}$$

The last term in equation (3) exists only when N is even. The Fourier coefficients $\bar{P}^{\text{"}k\text{"}\ell\text{"}}$ ("k" = 0; kc, ks, k = 1, 2, ..., k_L; N/2) in equation (3) do not vary from sector to sector, and are defined by

$$\left.\begin{aligned}
&\bar{P}^{0\text{"}\ell\text{"}} = \frac{1}{N}\sum_{n=1}^{N} P^{n\text{"}\ell\text{"}} \qquad (k = 0) \\
&\left.\begin{aligned}
\bar{P}^{k\text{"}\ell\text{"}c} &= \frac{2}{N}\sum_{n=1}^{N} P^{n\text{"}\ell\text{"}} \cos(\overline{n-1}ka) \\
\bar{P}^{k\text{"}\ell\text{"}s} &= \frac{2}{N}\sum_{n=1}^{N} P^{n\text{"}\ell\text{"}} \sin(\overline{n-1}ka), \quad \text{and}
\end{aligned}\right\} (k = 1, 2, \ldots, k_L) \\
&\bar{P}^{N/2\text{"}\ell\text{"}} = \frac{1}{N}\sum_{n=1}^{N} (-1)^{n-1} P^{n\text{"}\ell\text{"}} \ (N \text{ even only}) \quad (k = N/2) .
\end{aligned}\right\} \tag{5}$$

The terms $\overline{P}^{-"\ell"}_{"k"}$ ("ℓ" = 0; ℓc, ℓs, ℓ = 1, 2, ..., ℓ_L; M/2 and "k" = 0; kc, ks, k = 1, 2, ..., k_L; N/2) are the transformed frequency-dependent circumferential harmonic components of the directly applied loads p^m_n (m = 1, 2, ..., M and n = 1, 2, ..., N).

Directly applied loads (Circumferential harmonic-dependent and periodic in time).

Such loads can be represented as

$$\overline{P}^{m}_{"k"} = \overline{P}^{-0}_{"k"} + \sum_{\ell=1}^{\ell_L} \left[\overline{P}^{-\ell c}_{"k"} \cos(\overline{m-1}\ell b) + \overline{P}^{-\ell s}_{"k"} \sin(\overline{m-1}\ell b) \right] + (-1)^{m-1} \overline{P}^{-M/2}_{"k"} , \quad (6)$$

where m = 1, 2, ..., M represent the time instances at which harmonic components "k" = 0; kc, ks, k = 1, 2, ..., k_L; N/2 of directly applied loads are specified.

The coefficients $\overline{P}^{-"\ell"}_{"k"}$ on the right hand side of equation (6) are obtained using equations (2) with sector number n replaced by harmonic number "k".

Directly applied loads (frequency-and segment-dependent)

This type of loads can be represented as

$$p^{-"\ell"}_{n} = \overline{P}^{-"\ell"}_{o} + \sum_{k=1}^{k_L} \left[\overline{P}^{-"\ell"}_{kc} \cos(\overline{n-1}ka) + \overline{P}^{-"\ell"}_{ks} \sin(\overline{n-1}ka) \right] + (-1)^{n-1} \overline{P}^{-"\ell"}_{N/2} , \quad (7)$$

where "ℓ" (=1, 2, ..., F) now represents the frequencies at which excitation is specified. The transformed frequency-dependent circumferential harmonic components $\overline{P}^{-"\ell"}_{"k"}$ ("k" = 0; kc, ks, k = 1, 2, ..., k_L; N/2) are obtained using equations (5) with "ℓ" as defined above.

Directly applied loads (frequency- and circumferential harmonic-dependent)

These loads are the transformed frequency-dependent circumferential harmonic components $\overline{P}^{-"\ell"}_{"k"}$ ("k" = 0; kc, ks, k = 1, 2, ..., k_L; N/2) with "ℓ" (=1, 2, ..., F) representing the various frequencies at which the directly applied loads are specified.

Base acceleration (frequency- and circumferential harmonic-dependent)

In Appendix A, it is shown that the components of the translational base acceleration contribute to inertial loads on the rotating structure in the following manner:

ORIGINAL PAGE IS
OF POOR QUALITY

1. Axial component contributes to $\bar{P}^{"k"}_{-"\ell"}$ where "k" = 0, and "ℓ" represents the specified excitation frequencies.

2. Lateral components contribute to $\bar{P}^{"k"}_{-"\ell"}$ where "k" = 1c and 1s, and "ℓ" represents the <u>effective</u> excitation frequencies which are shifted from the specified frequencies by $\pm\,\Omega$, the rotational frequency.

2. <u>Application of Inter-Segment Compatibility Constraints</u>

As shown in Section 4.5.1 of Reference 7, equations (2) of Section 2 are used to derive the compatibility conditions relating the circumferential harmonic component degrees of freedom on the two sides of a rotationally cyclic sector:

$$\left.\begin{array}{lll} \underline{\text{side 2}} & \underline{\text{side 1}} & \\ \bar{u}_2^{o} = \bar{u}_1^{o} & & (k = o) \\ \left.\begin{array}{l} \bar{u}_2^{kc} = \bar{u}_1^{kc}\cos(ka) + \bar{u}_1^{ks}\sin(ka) \\ \bar{u}_2^{ks} = -\bar{u}_1^{kc}\sin(ka) + \bar{u}_1^{ks}\cos(ka) \end{array}\right\} & & (k = 1, 2, \ldots, k_L) \\ \text{and} \quad \bar{u}_2^{N/2} = -\bar{u}_1^{N/2}\,. & & (k = N/2) \end{array}\right\} \quad (8)$$

In order to apply these constraint relationships for any given harmonic k, an independent set $\bar{u}^{K}$ consisting of the circumferential harmonic component (cosine and sine) degrees of freedom from the interior and side 1 of the cyclic sector is defined. $\bar{u}^{K}$ is selected from the 'analysis' set degrees of freedom (i.e., the degrees of freedom retained after the application of constraints and any other reduction procedures), and is defined as

$$\left.\begin{array}{l} \bar{u}^{kc} = G_{ck}(k)\,\bar{u}^{K}, \quad \text{and} \\ \bar{u}^{ks} = G_{sk}(k)\,\bar{u}^{K} \quad . \end{array}\right\} \quad (9)$$

$\bar{u}^{kc}$ and $\bar{u}^{ks}$ each contain all (and only) the 'analysis' set degrees of freedom from the interior and <u>both</u> sides of the cyclic sector. Equations (8) are used to define some of the elements of the transformation matrices G_{ck} and G_{sk}. For k = o and N/2, the matrix G_{sk} is null.

ORIGINAL PAGE IS
OF POOR QUALITY

ORIGINAL PAGE IS
OF POOR QUALITY

3. Solution of Frequency-Dependent Harmonic Displacements

For a given harmonic k, the introduction of $\bar{u}^K$ in the equations of motion, equations (38), Section 2 , results in the transformed equations of motion (Ref. 1)

$$\bar{M}^K\ddot{\bar{u}}^K + \bar{B}^K\dot{\bar{u}}^K + \bar{K}^K\bar{u}^K = \bar{P}^K \quad , \tag{10}$$

where

$$\left.\begin{aligned} \bar{M}^K &= G_{ck}^T\, M^n\, G_{ck} + G_{sk}^T\, M^n\, G_{sk} \,, \\ \bar{B}^K &= G_{ck}^T\, B^n\, G_{ck} + G_{sk}^T\, B^n\, G_{sk} \,, \\ \bar{K}^K &= G_{ck}^T\, K^n\, G_{ck} + G_{sk}^T\, K^n\, G_{sk} \,, \text{ and} \\ \bar{P}^K &= G_{ck}^T\, \bar{P}^{kc} + G_{sk}^T\, \bar{P}^{ks} \quad . \end{aligned}\right\} \tag{11}$$

As discussed in subsection 1 of Section 3 , $\bar{P}^{kc}$ and $\bar{P}^{ks}$ are the transformed frequency-dependent circumferential harmonic components of the directly applied and base acceleration loads.

At any excitation frequency ω', let

$$\left.\begin{aligned} \bar{P}^K &= \bar{\bar{P}}^K e^{i\omega' t} \quad \text{and accordingly,} \\ \bar{u}^K &= \bar{\bar{u}}^K e^{i\omega' t} \quad , \end{aligned}\right\} \tag{12}$$

where $\bar{\bar{P}}^K$ and $\bar{\bar{u}}^K$ are complex quantities. Equation (10) can be rewritten as

$$[-\omega'^2\, \bar{M}^K + i\omega'\bar{B}^K + \bar{K}^K]\bar{\bar{u}}^K = \bar{\bar{P}}^K \quad . \tag{13}$$

The excitation frequency ω' is given by

$$\left.\begin{aligned} \omega' &= \omega \text{ for all directly applied and axial base acceleration} \\ &\qquad \text{loads, and} \\ &= \omega \pm \Omega \text{ for lateral base acceleration loads.} \end{aligned}\right\} \tag{14}$$

Equation (13) is solved for $\bar{\bar{u}}^K$ for all excitation frequencies and all harmonics as specified by the user. The cosine and sine harmonic components of displacements are recovered using equations (9) .

4. Recovery of Frequency-Dependent Displacements in Various Segments

This step is carried out only when the applied loads are specified on the various segments of the complete structure.

For loads specified as functions of time, equation (3) is used to obtain the displacements $\underline{u}^{"\ell"}_{n}$ in various segments with "ℓ" = 0; ℓc, ℓs, ℓ = 1, 2, ..., ℓ_{max}. The circumferential harmonic k is varied from k_{min} to k_{max}. The user specifies ℓ_{max}, k_{min} and k_{max}.

For loads specified as functions of frequency, equation (7) is used to obtain the displacements $\underline{u}^{"\ell"}_{n}$ in various segments with "ℓ" representing the excitation frequencies. The circumferential harmonic is varied from user specified k_{min} to k_{max}.

The solution procedure discussed in this section has been implemented as a new capability in NASTRAN (Ref. 8).

4. EXAMPLES

Five inter-related examples are presented to illustrate the theoretical development of the previous sections. The new capability added to NASTRAN to conduct forced vibration analysis of rotating cyclic structures (Ref. 8), as a result of the present development, has been used to conduct these examples. A 12-bladed disc is used for demonstration.

Example 1 is conducted on a finite element model of the complete structure (Figure 6). Examples 2 through 5 use a finite element model of one rotationally cyclic sector (Figure 7). Results of example 1 are used to verify some of the results obtained in the remaining examples. Table 1 summarizes the principal features demonstrated by these examples.

Steady-state frequency-dependent (sinusoidal) or time-dependent (periodic) loads are applied to selected grid point degrees of freedom. The specified loads can represent either the physical loads on various segments or their circumferential harmonic components. For illustration purposes only, the frequency band of excitation, 1700-1920 Hz, due to directly applied loads and base acceleration is selected to include the second bending mode of the disc for a circumferential harmonic index k = 2. The 'blade-to-blade' distribution of the directly applied loads also corresponds to k = 2. Table 2 lists the first few natural frequencies of the bladed disc for k = 0, 1 and 2. Modes for k = 2 are shown in Figure 8.

<u>General Input</u>

1. Parameters:

Diameter at blade tip	=	19.4 in.
Diameter at blade root	=	14.2 in.
Shaft diameter	=	4.0 in.
Disc thickness	=	0.25 in.
Blade thickness	=	0.125 in.
Young's modulus	=	30.0×10^6 lbf/in^2
Poisson's ratio	=	0.3
Material density	=	7.4×10^{-4} lbf-sec^2/in^4
Uniform structural damping (g)	=	0.02

2. Constraints:

All constraints are applied in <u>body-fixed</u> global coordinate system(s). All grid points on the shaft diameter are completely fixed. Rotational degrees of freedom θ_Z at remaining grid points are constrained to zero.

ORIGINAL PAGE IS
OF POOR QUALITY

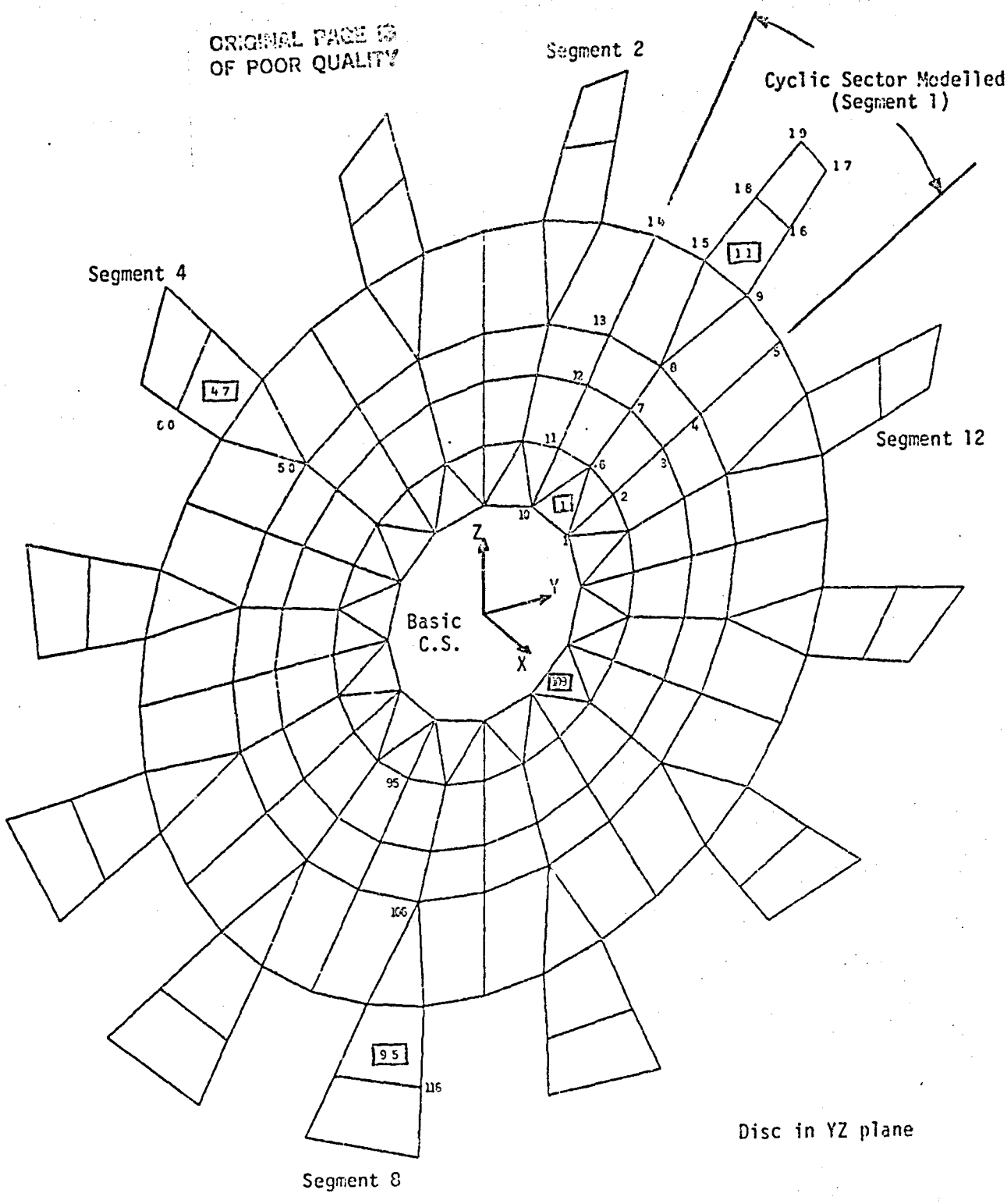

Figure 6: NASTRAN Model of the 12-Bladed Disc

ORIGINAL PAGE IS
OF POOR QUALITY

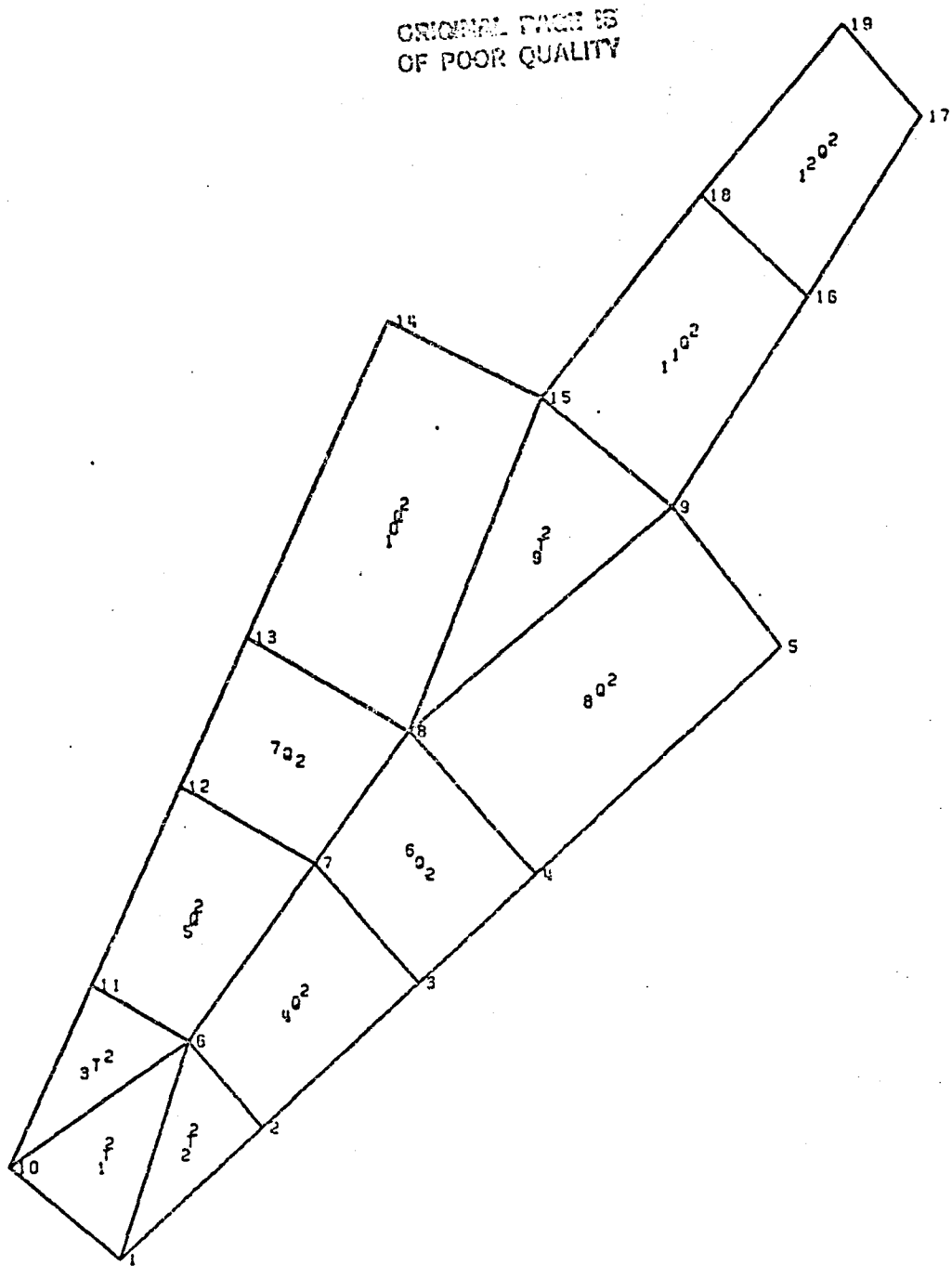

Figure 7: NASTRAN Cyclic Model of the 12-Bladed Disc

TABLE 1: PRINCIPAL FEATURES DEMONSTRATED BY EXAMPLE PROBLEMS

Example No.	Finite Element Model of	Applied loads specified as functions of				Base Acceleration	Rotational Speed
		Frequency (sinusoidal)		Time (periodic)			
		Physical Components	Circum.Harmonic Components	Physical Components	Circum.Harmonic Components		
1	Complete Structure	Yes				No	No
2	Cyclic Sector	Yes				No	No
3	Cyclic Sector		Yes			Yes	Yes
4	Cyclic Sector			Yes		No	Yes
5	Cyclic Sector				Yes	No	Yes

ORIGINAL PAGE IS
OF POOR QUALITY

ORIGINAL PAGE IS
OF POOR QUALITY

TABLE 2: BLADED-DISC NATURAL FREQUENCIES

Frequency (Mode No.), Hz.			Mode Description
k* = 0	k = 1	k = 2	
214 (1)	208 (1)	242 (1)	
591 (2)	594 (2)	622 (2)	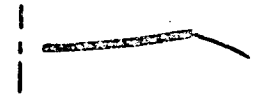
1577 (3)	1633 (3)	1814 (3)	
2468 (5)**	2460 (4)	2433 (4)	

* k is the circumferential harmonic index

** Mode No. 4 for k = 0 at 1994 Hz represents an in-plane shear mode not excited by the applied forces.

ORIGINAL PAGE IS
OF POOR QUALITY

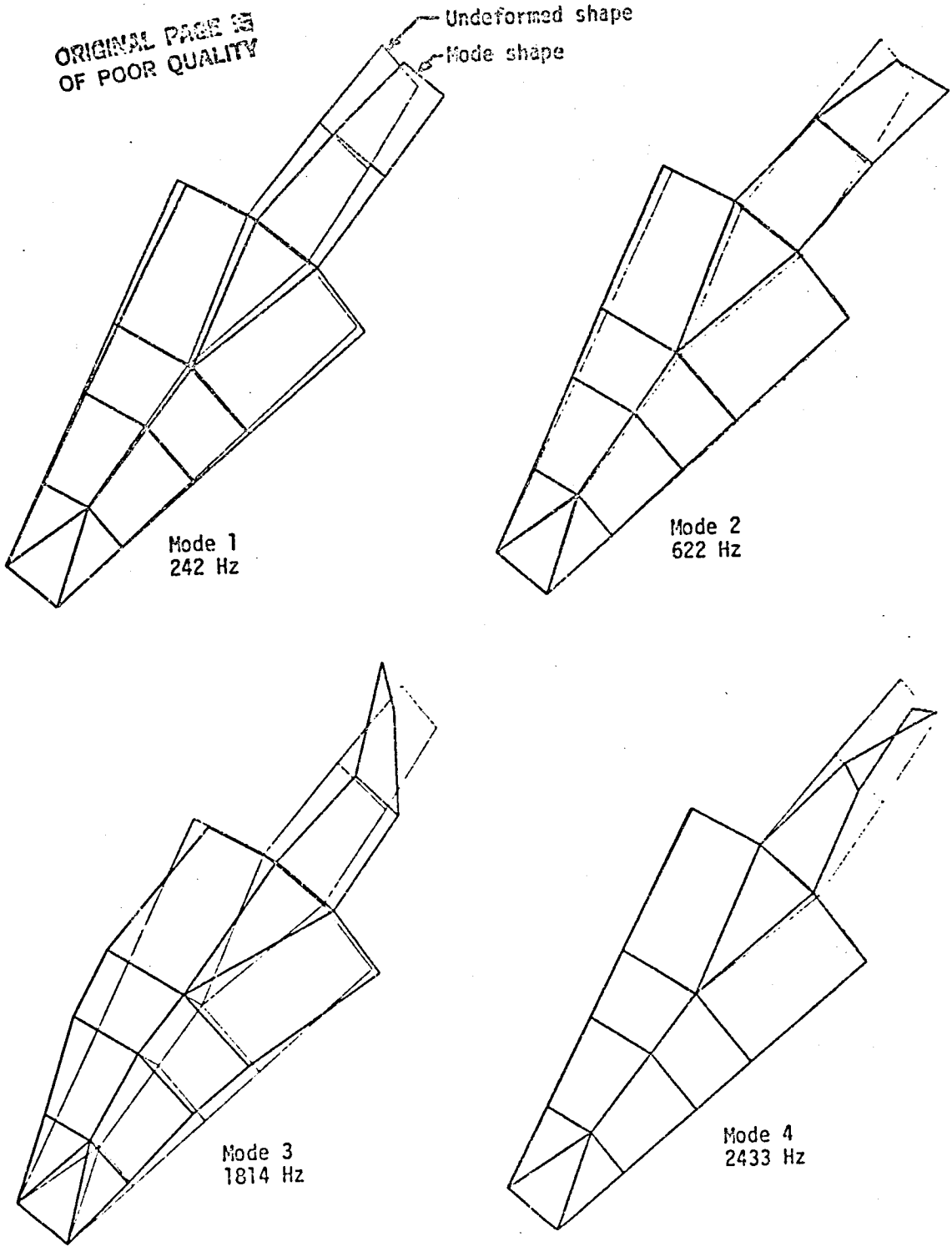

Figure 8: k = 2 Modes of Bladed Disc

EXAMPLE 1

Description

This example uses the direct frequency response capability in NASTRAN, RF8, and forms the basis to verify some of the results of examples 2 through 5.

Input

1. Parameters:

   Same as general input parameters.

2. Constraints:

   Same as general input constraints.

3. Loads:

$$P(f;n) = A(f) \cos\left(\overline{n-1} \cdot 2 \cdot \frac{2\pi}{12}\right) ,$$

where n is the segment number,
2 represents k = 2,
12 represents the total number of segments in the bladed disc.
P is specified using RLOADi bulk data cards.

Results

Sample plots of grid point displacement and element stress response are shown in Figures 9 through 11. The expected behavior about a k = 2 natural frequency of the bladed disc can be seen in all these figures.

All the response plots (Figures 9 through 25 except 16) have been obtained using the plotting capability of NASTRAN. On any given plot, the various curves are identified, in order, by symbols X, *, +, -, • and o. The sequence of curves is indicated in the first line of the plot description at the bottom left of each figure.

ORIGINAL PAGE IS
OF POOR QUALITY

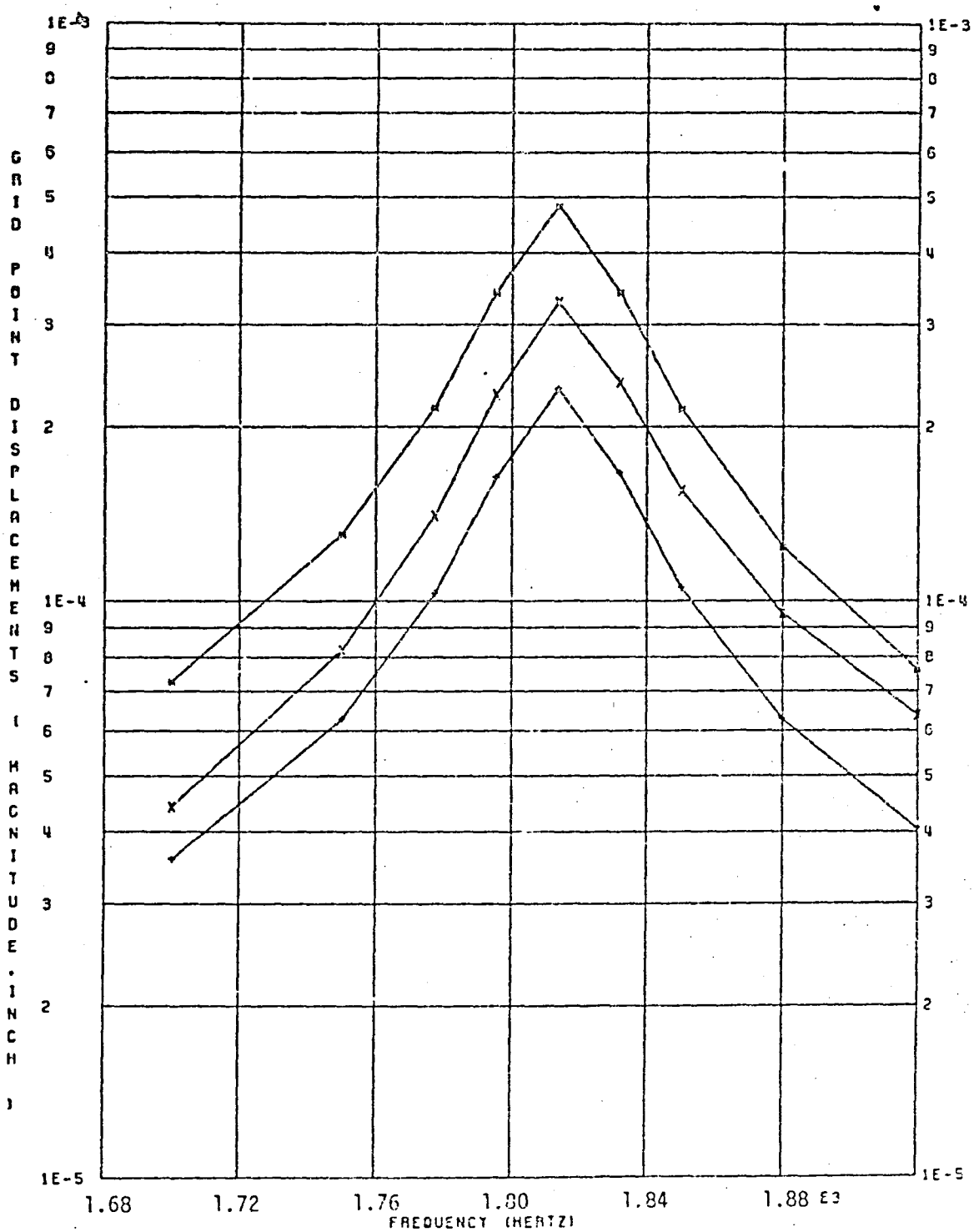

14(T3RM),18(T3RM),95(T3RM)
FORCED VIBRATION ANALYSIS OF ROTATING CYCLIC STRUCTURES
BLADED DISC EXAMPLE 1 (FULL MODEL,FREQ LOADS)
KINDEX 2C TYPE LOADS

Figure 9

ORIGINAL PAGE IS
OF POOR QUALITY

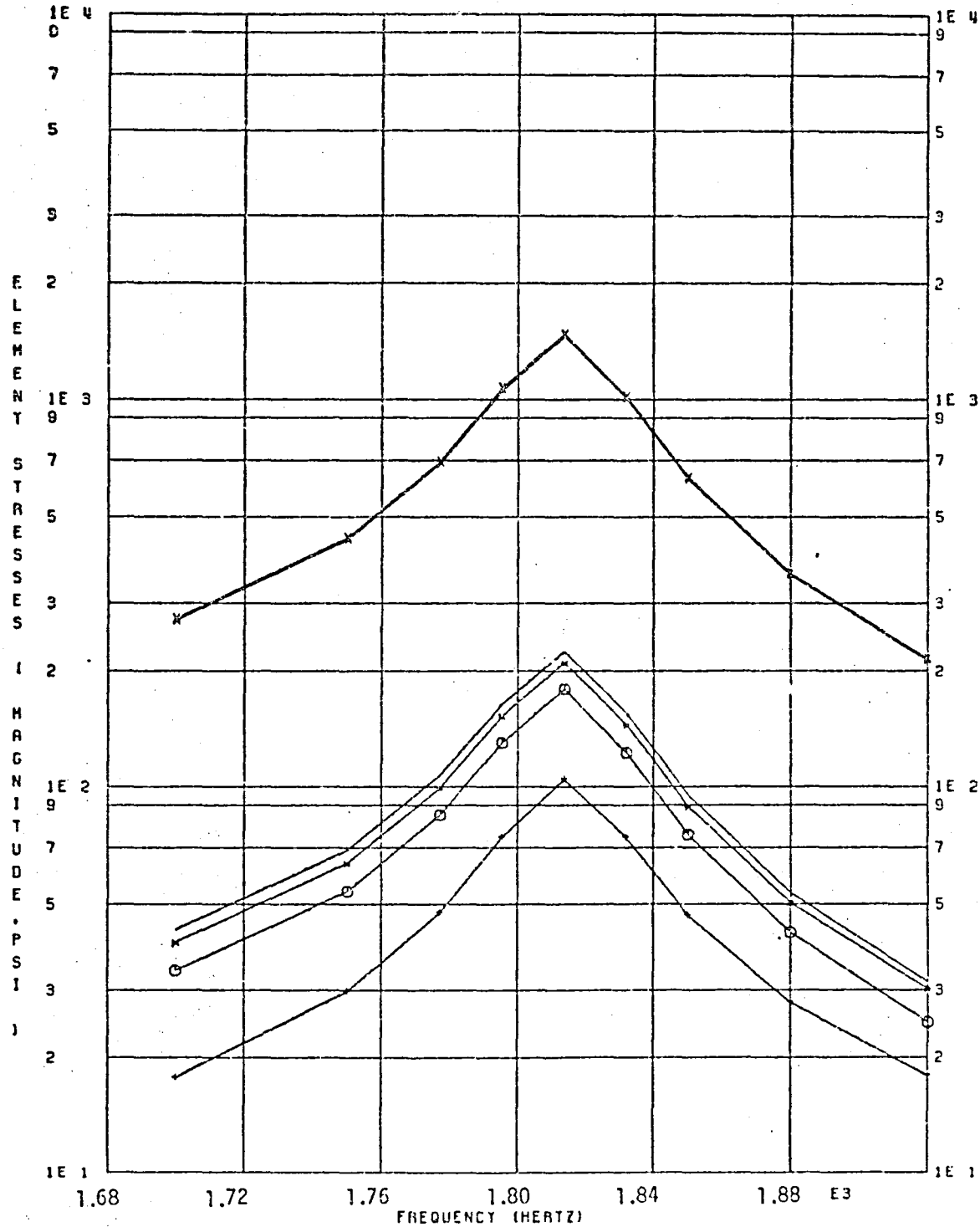

11(3),11(5),11(7),11(10),11(12),11(14)
FORCED VIBRATION ANALYSIS OF ROTATING CYCLIC STRUCTURES
BLADED DISC EXAMPLE 1 (FULL MODEL,FREQ LOADS)
KINDEX 2C TYPE LOADS

Figure 10

ORIGINAL PAGE IS
OF POOR QUALITY

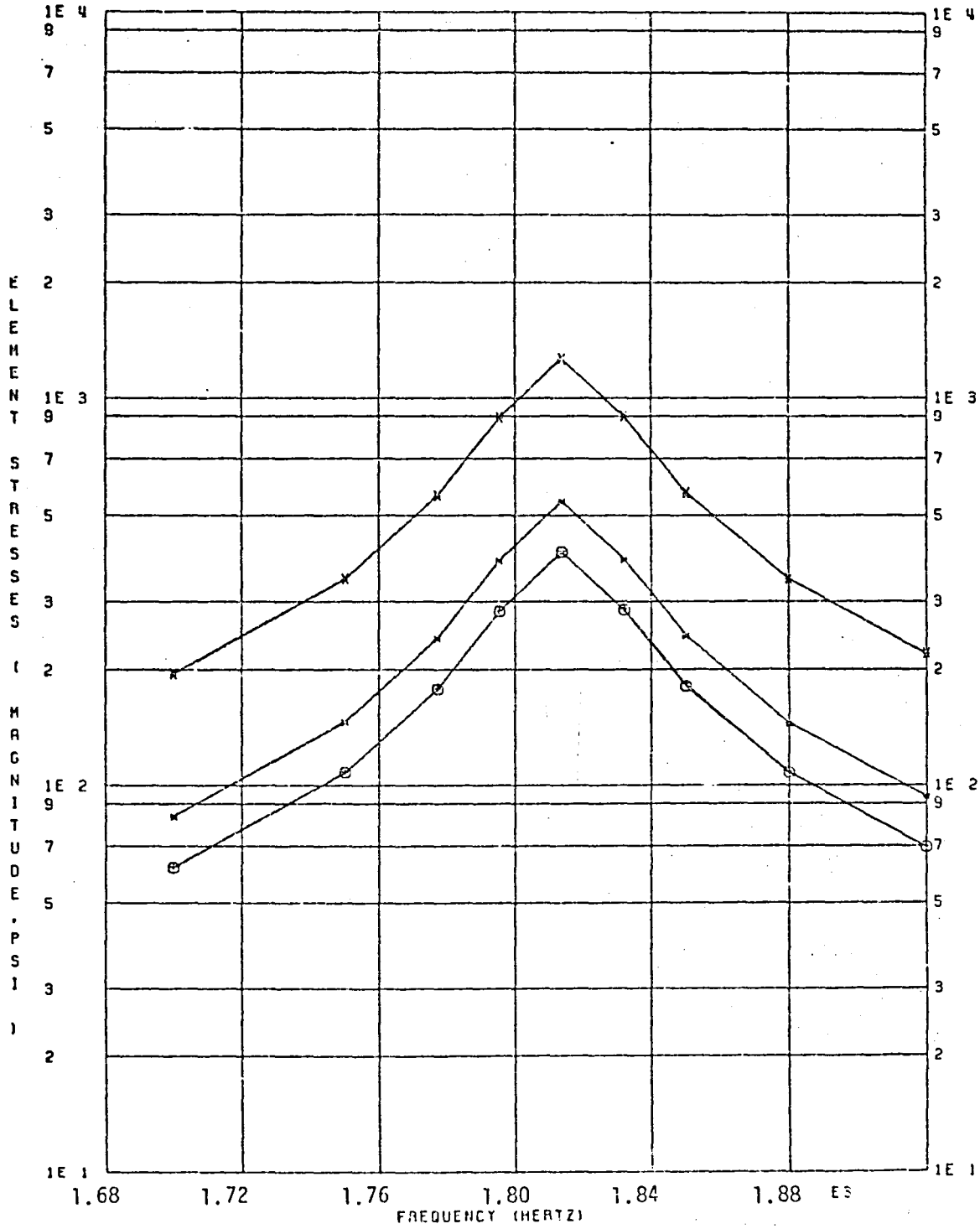

109(3),109(5),109(7),109(10),109(12),109(14)
FORCED VIBRATION ANALYSIS OF ROTATING CYCLIC STRUCTURES
BLADED DISC EXAMPLE 1 (FULL MODEL,FREQ LOADS)
KINDEX 2C TYPE LOADS

Figure 11

EXAMPLE 2

Description

This example uses the forced vibration capability with cyclic symmetry. The user input/output data for loads, displacements, stresses, etc., pertain to the physical representation of the various segments of the bladed disc. The frequency-dependent applied loads correspond to k = 2, and hence the solution loops on the circumferential harmonic index k are restricted to k = 2 only via parameters KMIN and KMAX.

Input

1. Parameters:

   In addition to general input parameters,

   CYCIO = +1 physical cyclic input/output data
   KMIN = 2 minimum circumferential harmonic index
   KMAX = 2 maximum circumferential harmonic index
   NSEGS = 12 number of rotationally cyclic segments
   RPS = 0.0 rotational speed
   GKAD = FREQRESP } Specify the form in which the damping parameters
   LGKAD = +1 } are used.

2. Constraints:

   Same as general input constraints.

3. Loads:

$$P^n(f) = A(f) \cos\left(\overline{n-1} \cdot 2 \cdot \frac{2\pi}{12}\right) ,$$

where n is the segment number,
2 represents k = 2,
12 represents the total number of segments in the bladed disc.
P is specified using RLOADi bulk data cards.

Results

Displacement and stress output results for selected grid points and elements are presented in Figures 12 through 15. Agreement between results of Figures 12-13 and Figure 9, Figure 14 and Figure 10, and Figure 15 and Figure 11 is excellent.

ORIGINAL PAGE IS
OF POOR QUALITY

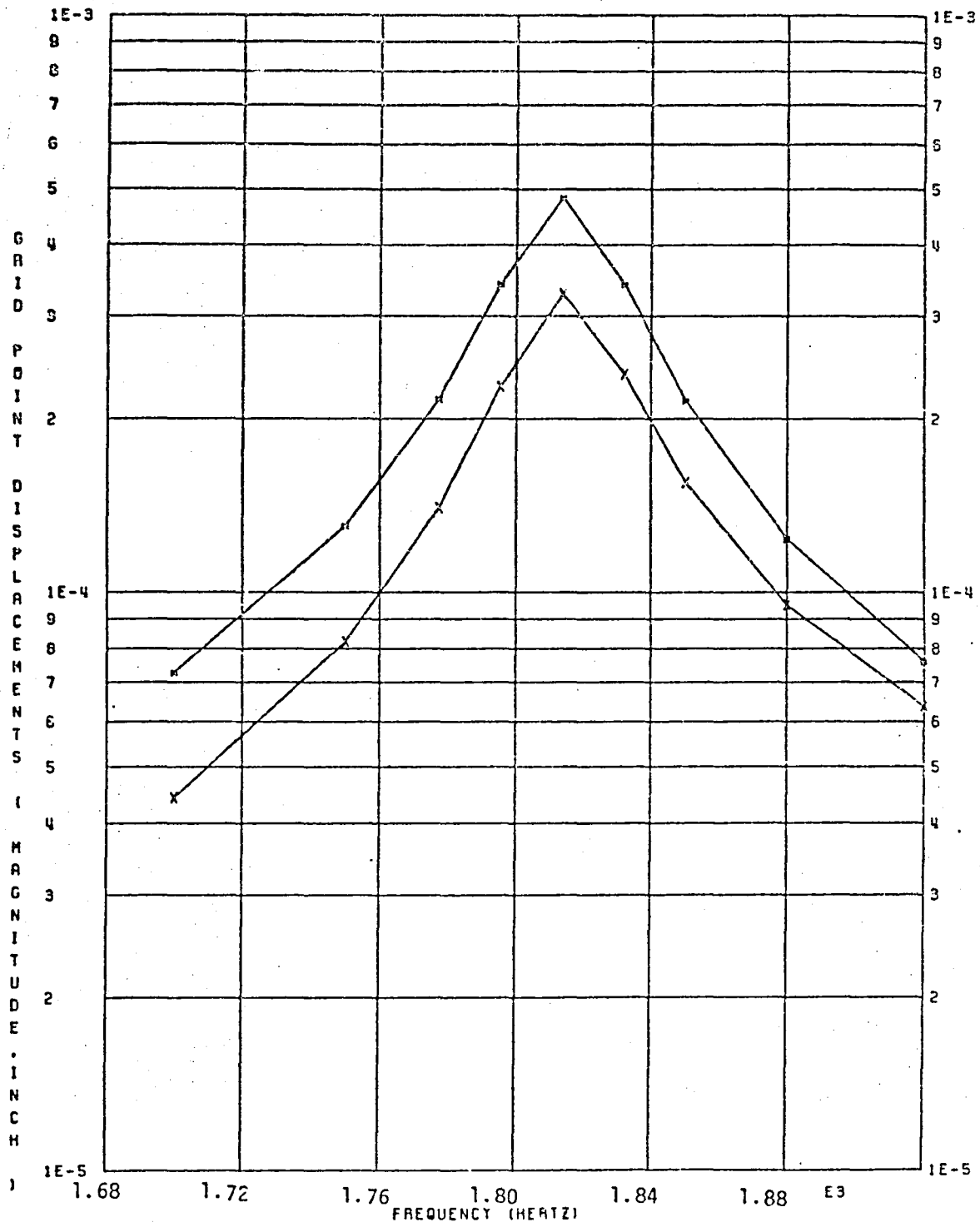

14(T3RM),18(T3RM)
FORCED VIBRATION ANALYSIS OF ROTATING CYCLIC STRUCTURES
BLADED DISC EXAMPLE 2 (CYC MODEL,FREQ LOADS,PHYSICAL I/O)
SEGMENT 1 SUBCASE 1

Figure 12

ORIGINAL PAGE IS
OF POOR QUALITY

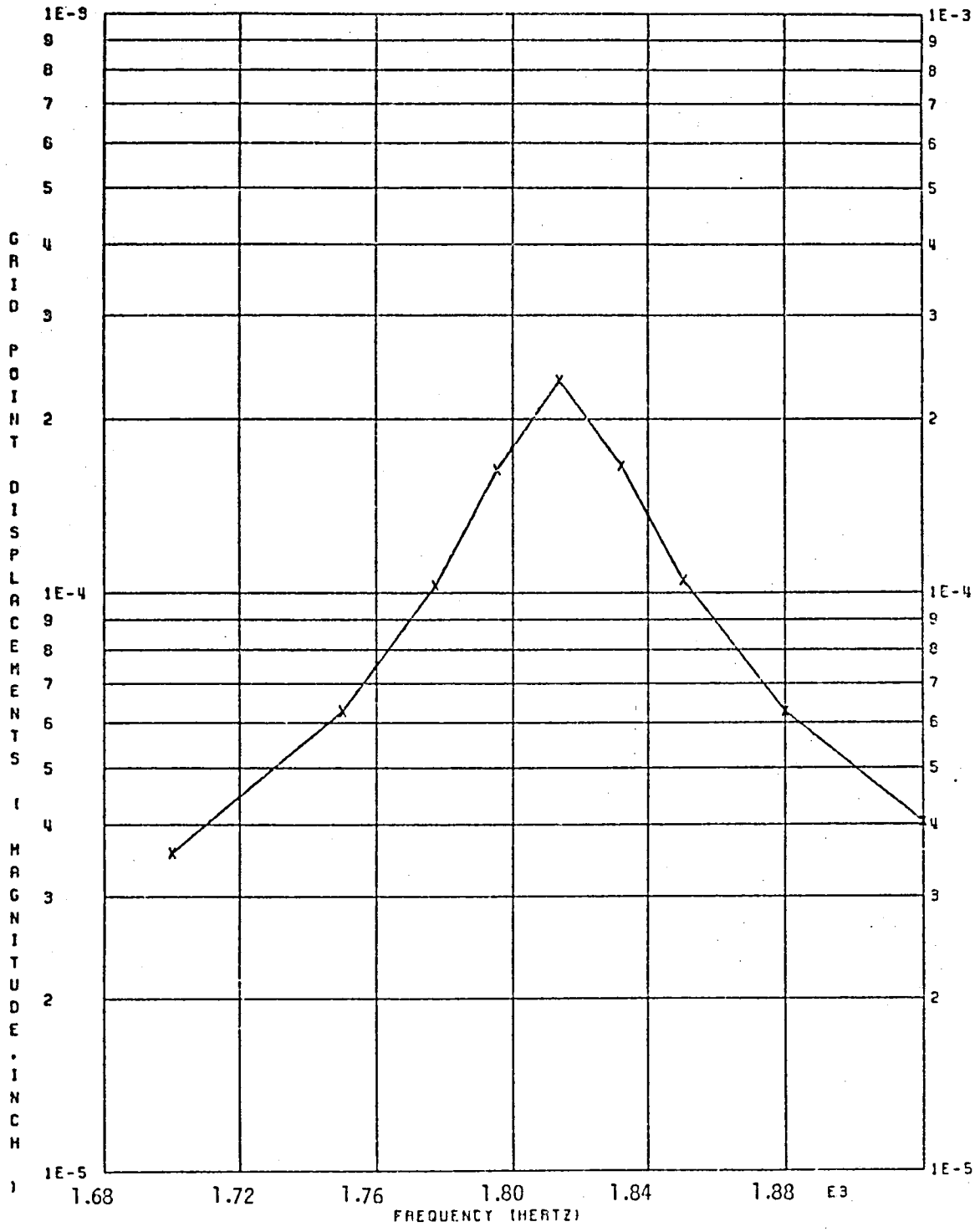

2(T3RM)
FORCED VIBRATION ANALYSIS OF ROTATING CYCLIC STRUCTURES
BLADED DISC EXAMPLE 2 (CYC MODEL,FREQ LOADS,PHYSICAL I/O)
SEGMENT 8 SUBCASE 8

Figure 13

ORIGINAL PAGE IS
OF POOR QUALITY

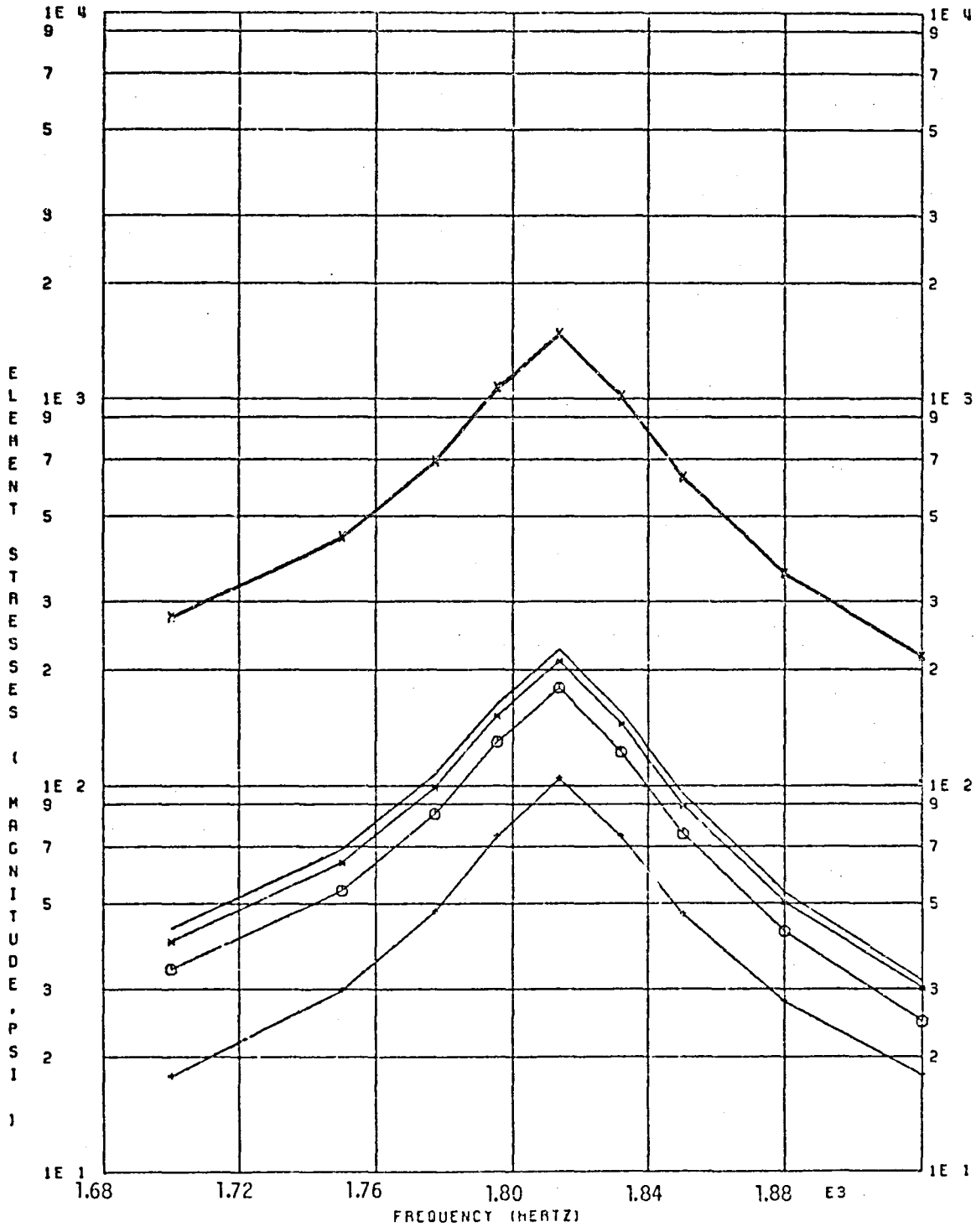

11(3),11(5),11(7),11(10),11(12),11(14)
FORCED VIBRATION ANALYSIS OF ROTATING CYCLIC STRUCTURES
BLADED DISC EXAMPLE 2 (CYC MODEL,FREQ LOADS,PHYSICAL I/O)
SEGMENT 1 SUBCASE 1

Figure 14

ORIGINAL PAGE IS
OF POOR QUALITY

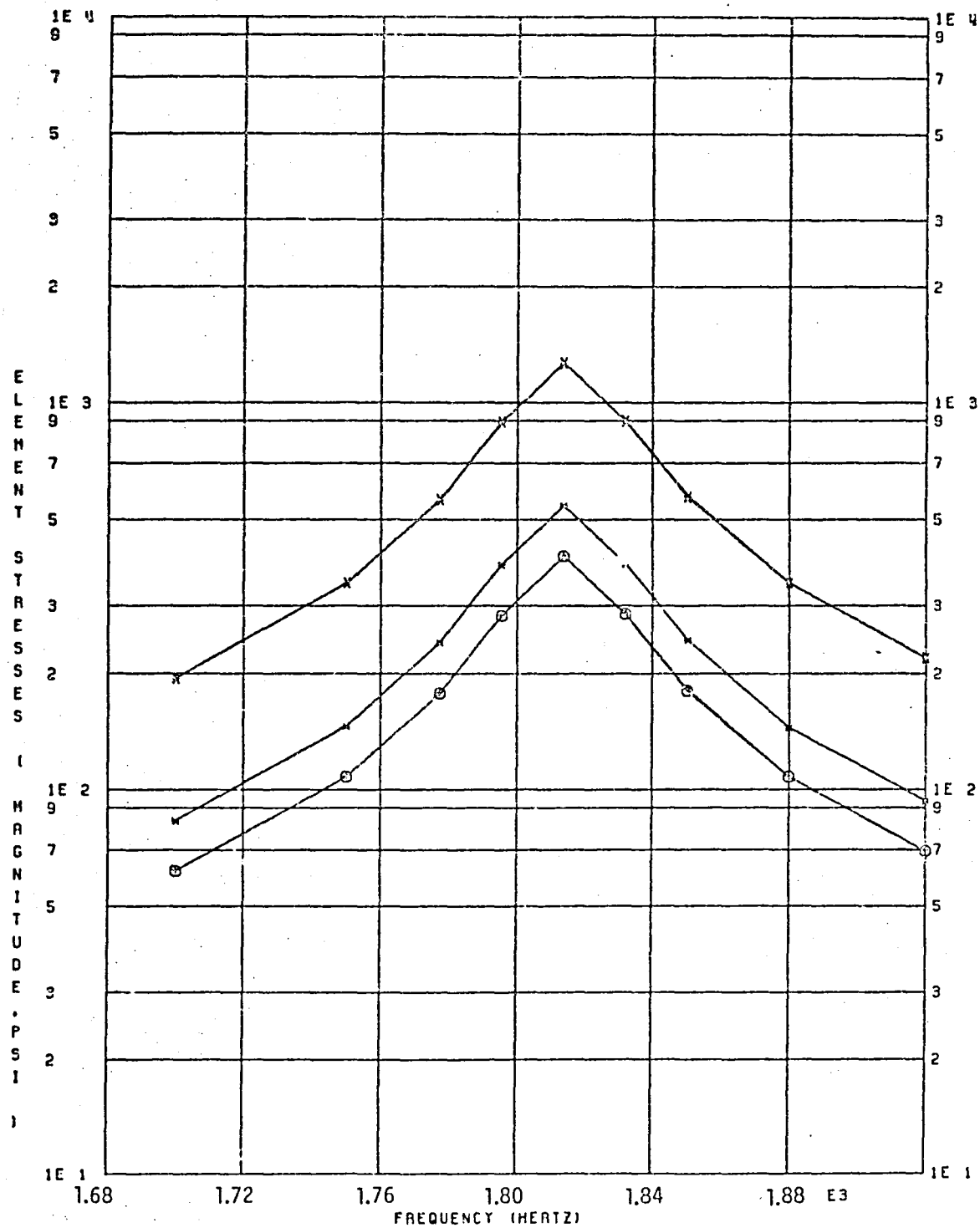

1(3),1(5),1(7),1(10),1(12),1(14)
FORCED VIBRATION ANALYSIS OF ROTATING CYCLIC STRUCTURES
BLADED DISC EXAMPLE 2 (CYC MODEL,FREQ LOADS,PHYSICAL I/O)
SEGMENT 10 SUBCASE 10

Figure 15

EXAMPLE 3

Description

This example uses the forced vibration capability with cyclic symmetry. The user input/output data pertain to harmonic representation. Frequency-dependent excitation is provided by both directly applied and base acceleration loads.

Input

1. Parameters:

   In addition to general input parameters,

   CYCIO = -1 harmonic cyclic input/output data
   KMIN = 0 minimum circumferential harmonic index
   KMAX = 2 maximum circumferential harmonic index
   NSEGS = 12 number of rotationally cyclic sectors
   RPS = 600.0 revolutions per second
   BXTID, BYTID, BZTID } Refer to TABLEDi bulk data cards to specify
   BXPTID, BYPTID, BZPTID } magnitude and phase of base acceleration components.
   GKAD = FREQRESP } Specify the form in which damping parameters are
   LGKAD = +1 } used.

2. Constraints:

   Same as general input constraints.

3. Loads:

   a) $\overline{P}^{0,2c} = A(f)$ specified on RLOADi bulk data cards.
   b) Base acceleration as shown in Figure 16 .

Results

Results are shown in Figures 17 through 25.

Figures 17 and 18 present k = 0 results (subcase 1). The excitation consists of axial base acceleration and directly applied loads. The selected frequency band of excitation, 1700-1920 Hz, lies between the second out-of-plane disc bending mode frequency (1577 Hz, k = 0, Table 2) and the first in-plane shear mode frequency (1994 Hz, k = 0, Table 2). Since the excitation is parallel to the axis of rotation, only the former mode responds.

Figures 19 through 23 present k = 1 results (subcases 2 (k = 1c) and 3 (k = 1s)). The excitation is due to lateral base acceleration only. Although the frequency band of input base acceleration is 1700-1920 Hz, the rotation of the bladed disc at 600 Hz (parameter RPS) splits the input bandwidth into two effective bandwidths:

$$(1700 - 600) = \underline{1100} \text{ to } (1920 - 600) = \underline{1320} \text{ Hz, and}$$
$$(1700 + 600) = \underline{2300} \text{ to } (1920 + 600) = \underline{2520} \text{ Hz.}$$

The only k = 1 mode in these effective bandwidths is the first torsional mode of the blade with the disc practically stationary (2460 Hz, k = 1, Table 2). This is shown by the out-of-plane displacement magnitudes of grid points 18 (blade) and 8 (disc) respectively (Figures 19 (k = 1c) and 22 (k = 1s)). The corresponding phase responses of these grid points are shown in Figure 21.

Figures 24 and 25 present k = 2 results (subcase 4 (k = 2c)). The excitation consists of directly applied k = 2c loads. The out-of-plane displacement magnitude of grid point 18 (Figure 24) compares well with that obtained in example 2 (Figure 12). Table 3 lists the out-of-plane displacement response of grid point 18 as obtained in examples 2 and 3. The marginal difference in response in example 3 is due to the Coriolis and centripetal acceleration effects at a rotational speed of 600 revolutions per second.

No k = 2s loads are applied in this example (subcase 5).

ORIGINAL PAGE IS
OF POOR QUALITY

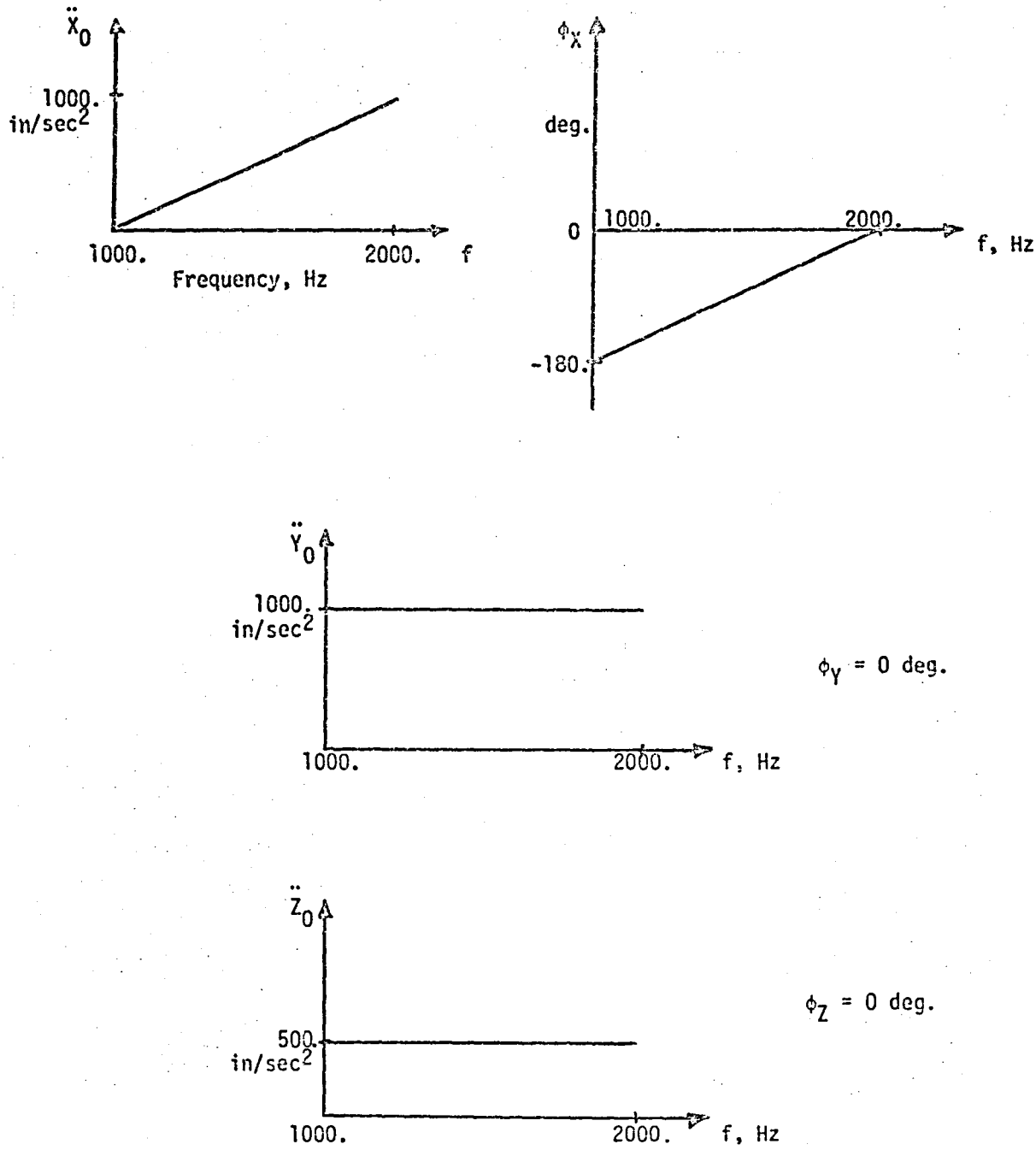

Figure 16: Base Acceleration Data in an Inertial Coordinate System

ORIGINAL PAGE IS
OF POOR QUALITY

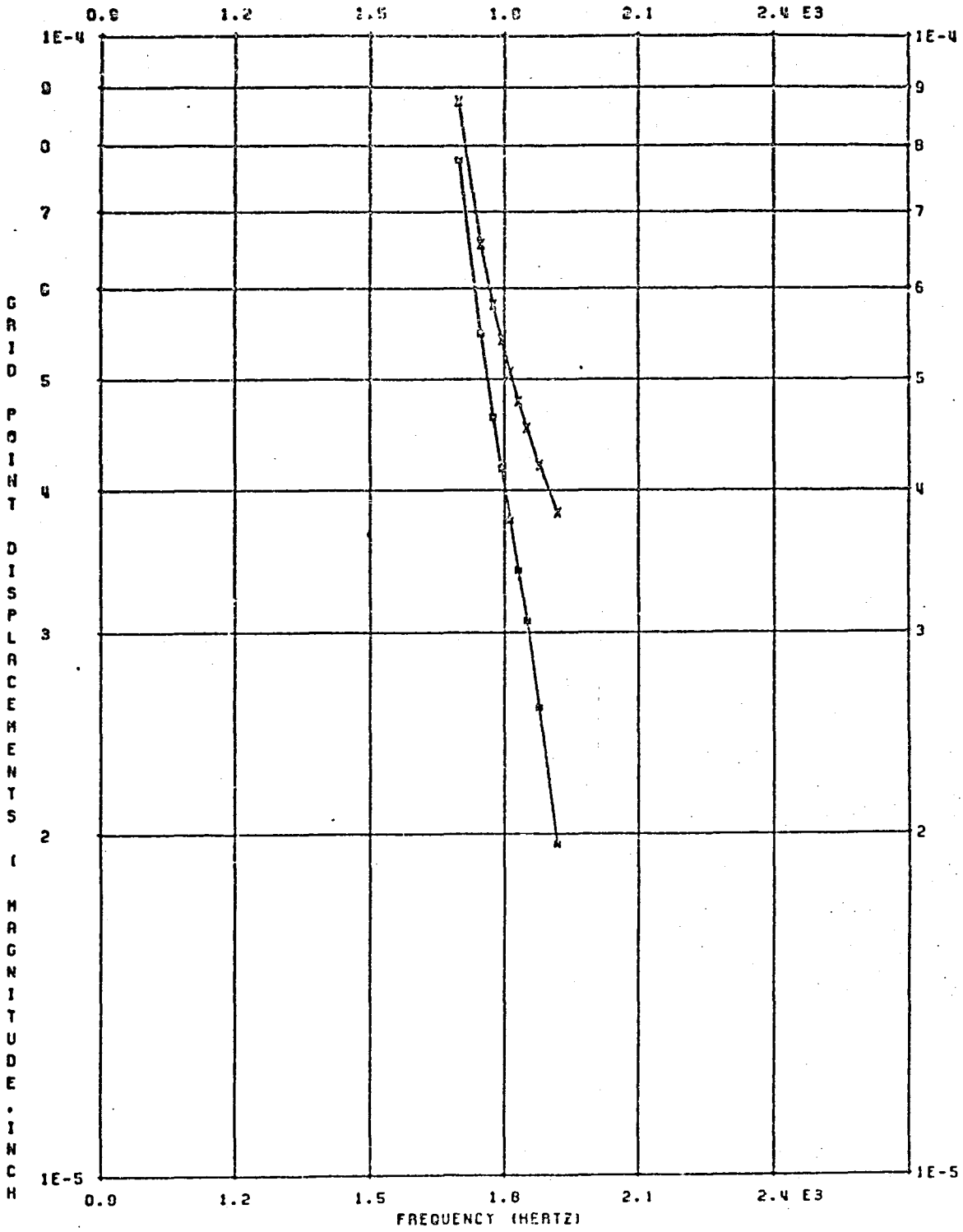

8(T3RH),18(T3RH)
FORCED VIBRATION ANALYSIS OF ROTATING CYCLIC STRUCTURES
BLADED DISC EXAMPLE 3 (CYC MODEL,FREQ+BASE RCCN LOAD,HARM I/O
KINDEX 0 SUBCASE 1

Figure 17

ORIGINAL PAGE IS
OF POOR QUALITY

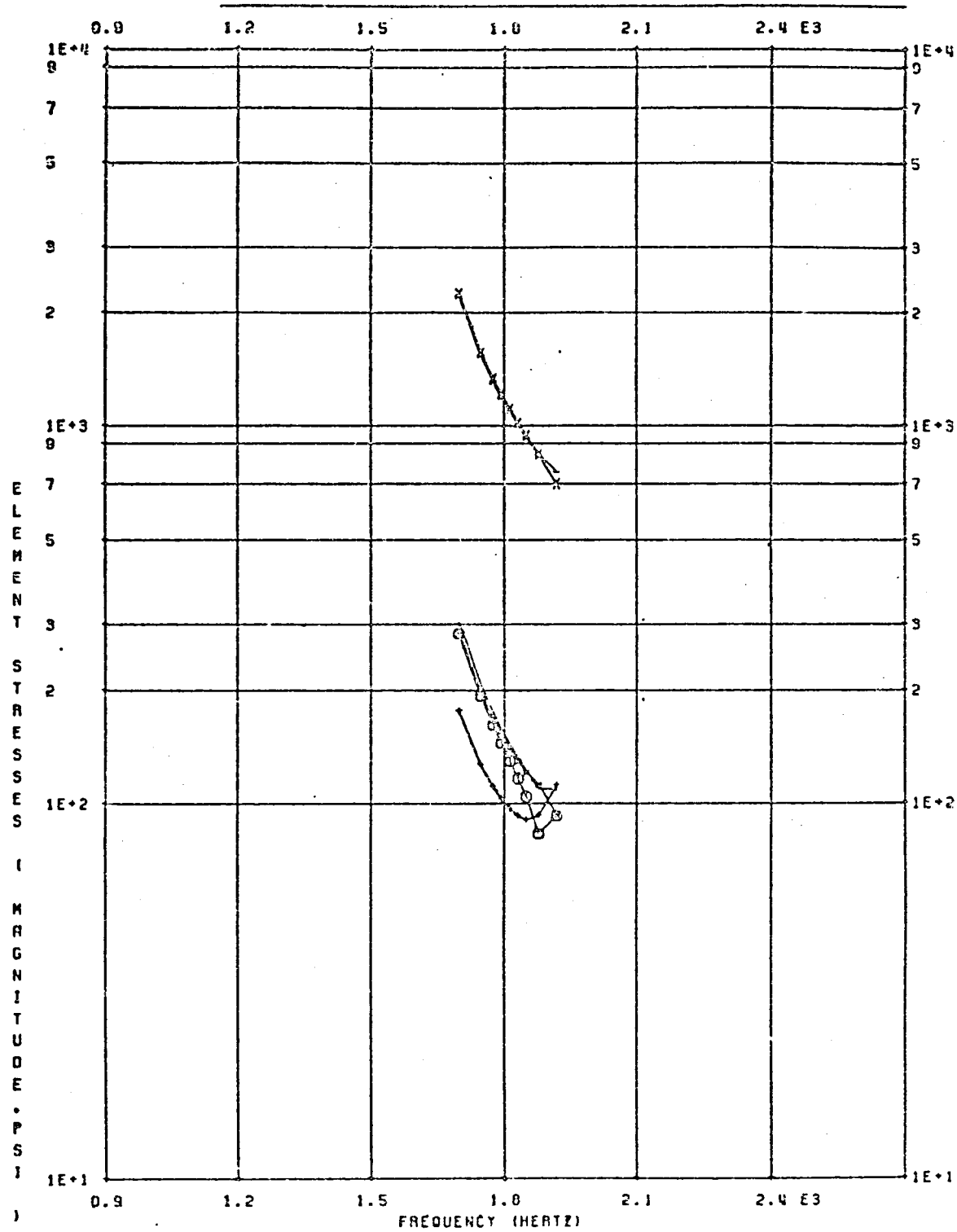

11(3),11(5),11(7),11(10),11(12),11(14)
FORCED VIBRATION ANALYSIS OF ROTATING CYCLIC STRUCTURES
BLADED DISC EXAMPLE 3 (CYC MODEL,FREQ+BASE ACCN LOAD,MARK I/O
KINDEX 0 SUBCASE 1

Figure 18

ORIGINAL PAGE IS
OF POOR QUALITY

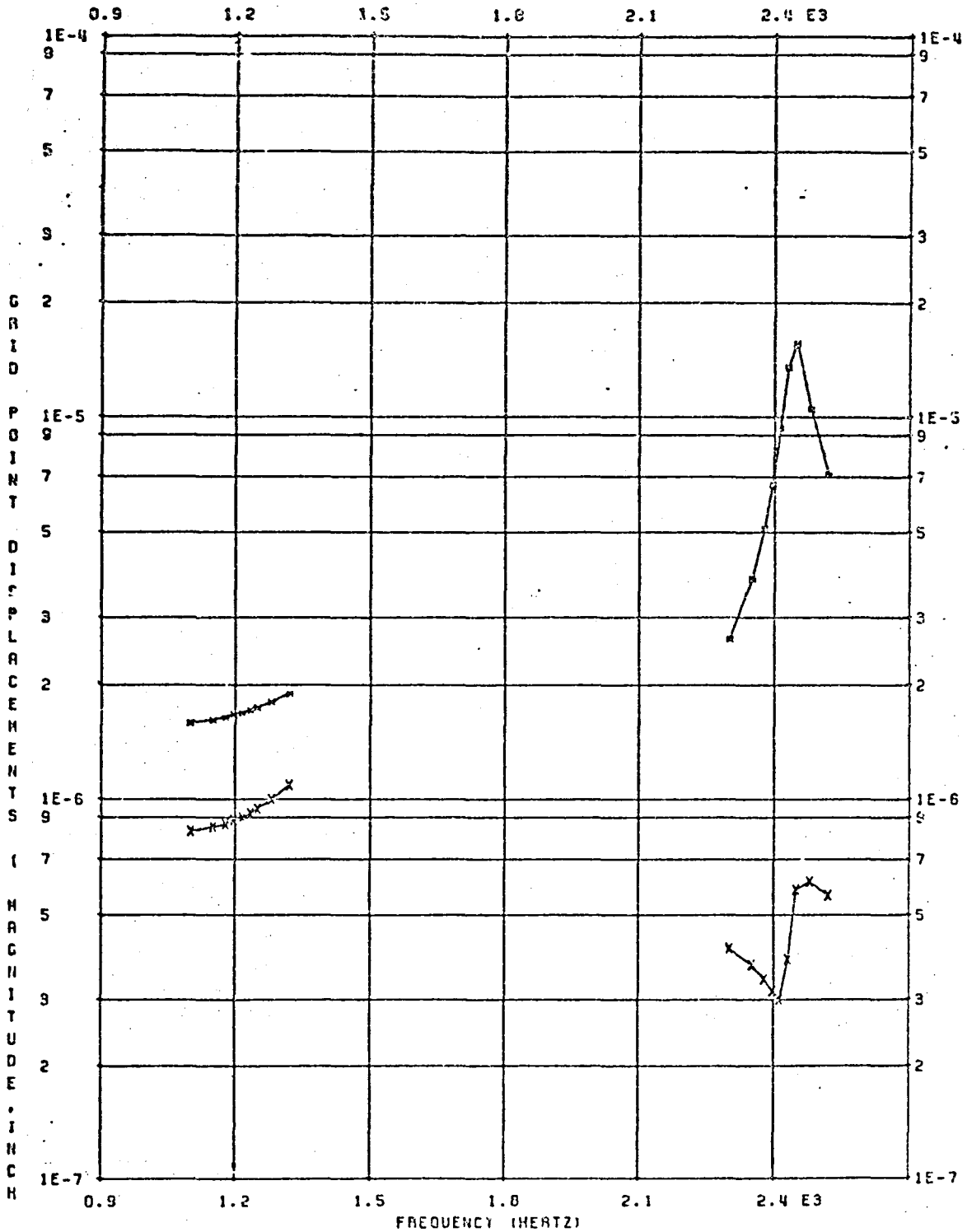

8(T3RM),18(T3RM)
FORCED VIBRATION ANALYSIS OF ROTATING CYCLIC STRUCTURES
BLADED DISC EXAMPLE 3 (CYC MODEL,FREQ+BASE ACCN LOAD,HARM I/O
KINDEX 1C SUBCASE 2

Figure 19

ORIGINAL PAGE IS
OF POOR QUALITY

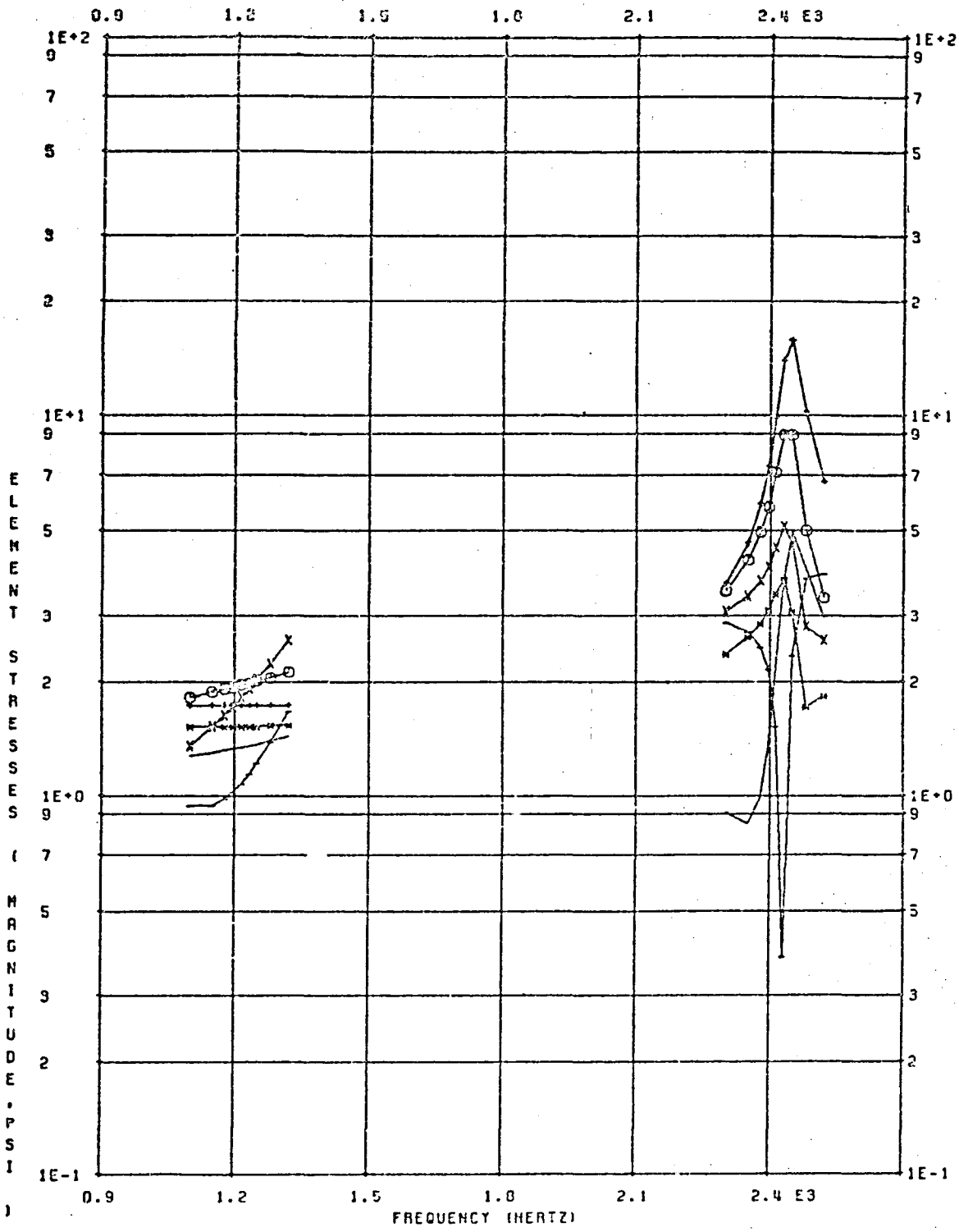

11(3),11(5),11(7),11(10),11(12),11(14)
FORCED VIBRATION ANALYSIS OF ROTATING CYCLIC STRUCTURES
BLADED DISC EXAMPLE 3 (CYC MODEL,FREQ+BASE ACCN LOAD,HARM I/O
KINDEX 1C SUBCASE 2

Figure 20

ORIGINAL PAGE IS
OF POOR QUALITY

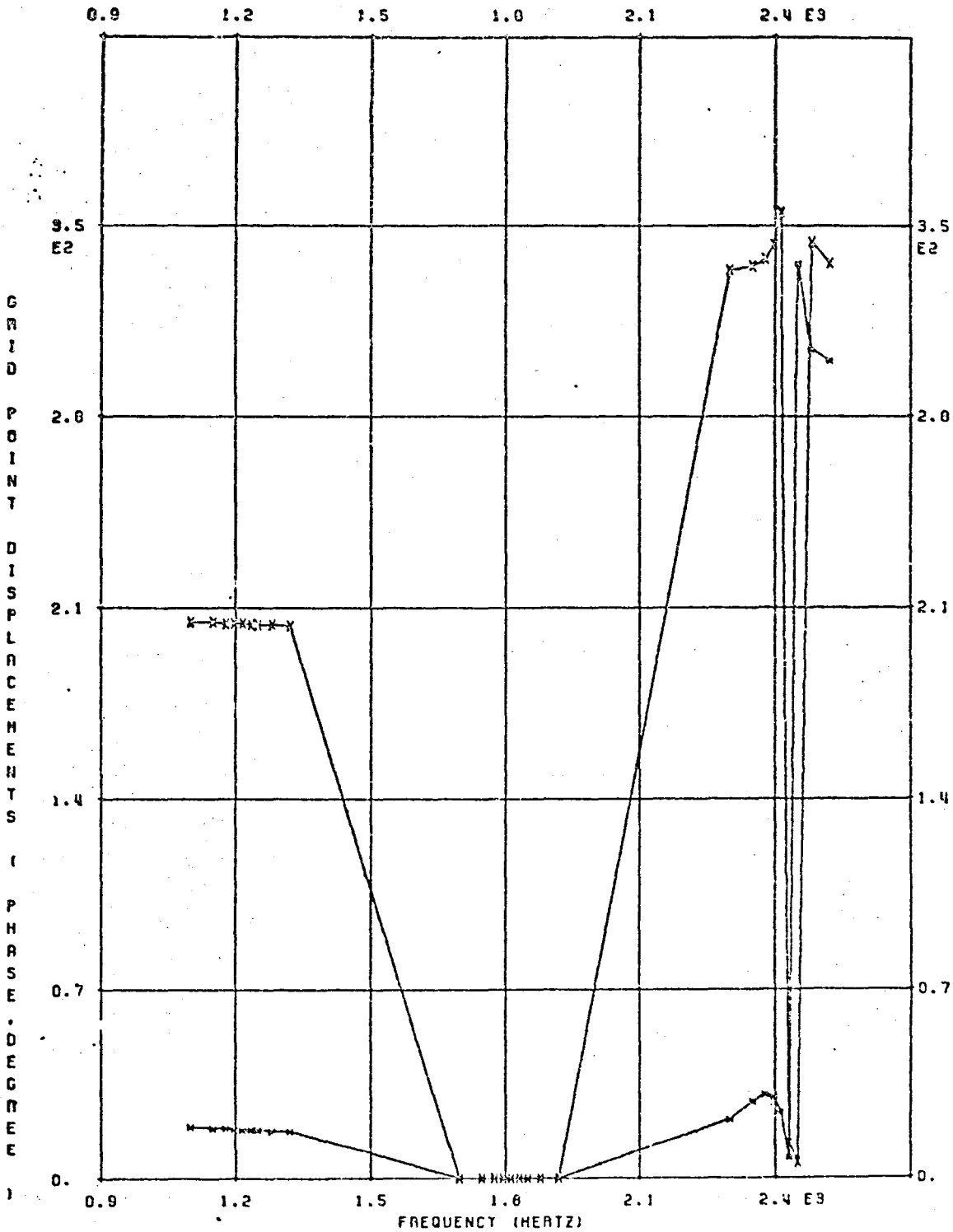

B(T3IP),18(T3IP)
FORCED VIBRATION ANALYSIS OF ROTATING CYCLIC STRUCTURES
BLADED DISC EXAMPLE 3 (CYC MODEL,FREQ+BASE ACCN LOAD,HARM I/O
KINDEX 1C SUBCASE 2

Figure 21

ORIGINAL PAGE IS
OF POOR QUALITY

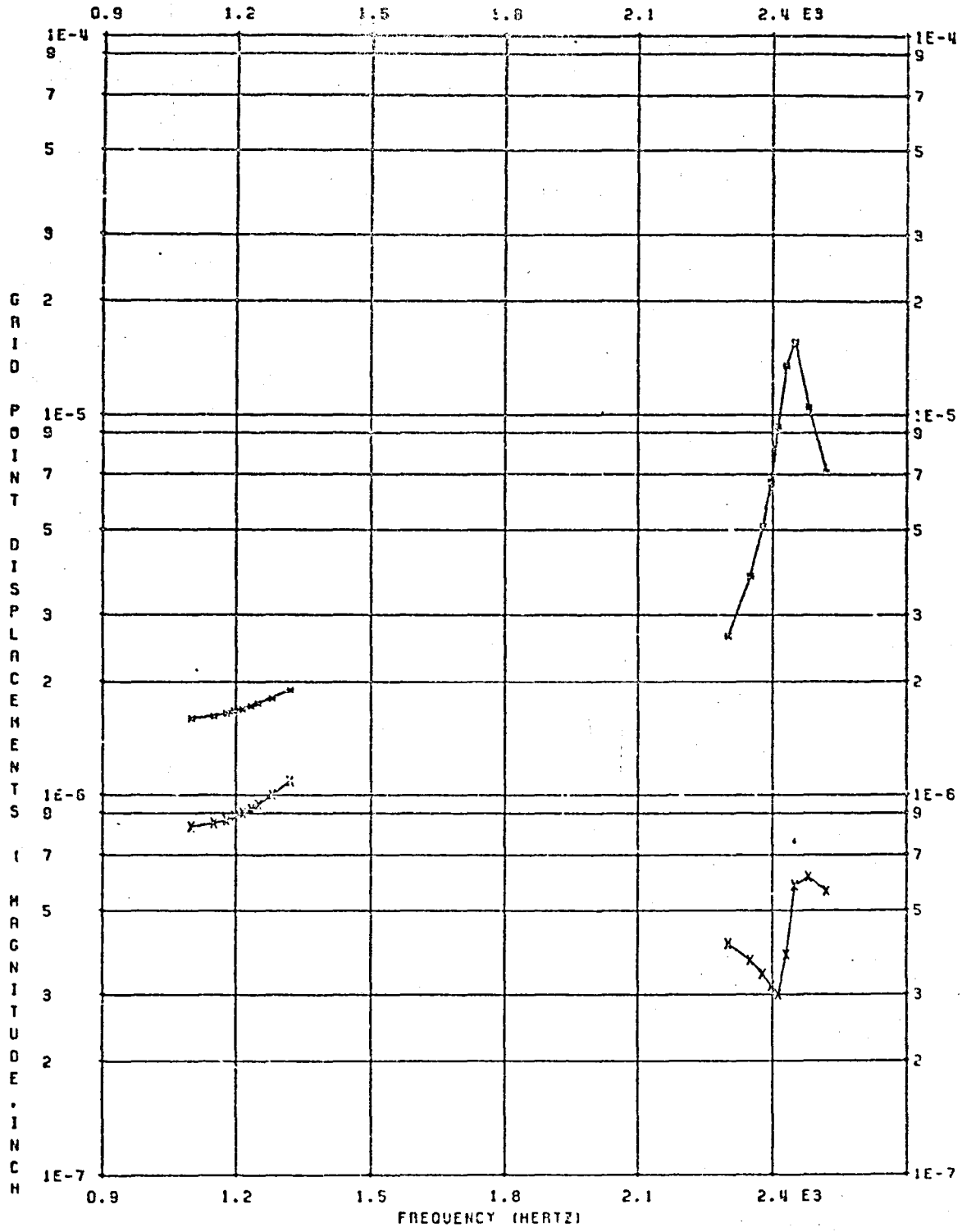

6(T3RM),18(T3RM)
FORCED VIBRATION ANALYSIS OF ROTATING CYCLIC STRUCTURES
BLADED DISC EXAMPLE 3 (CYC MODEL,FREQ+BASE ACCN LOAD,HARM I/O
KINDEX 15 SUBCASE 3

Figure 22

ORIGINAL PAGE IS
OF POOR QUALITY

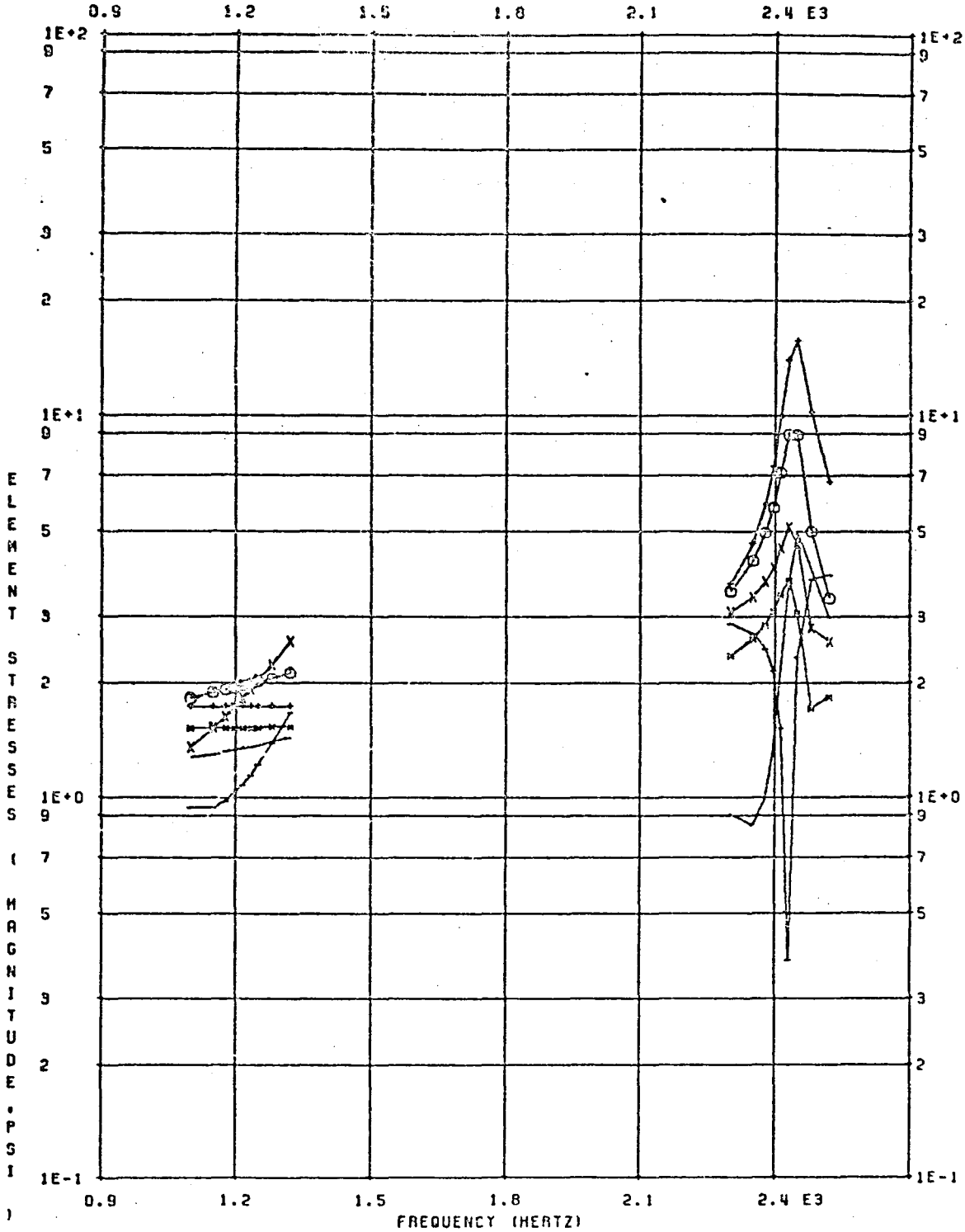

11(3),11(5),11(7),11(10),11(12),11(14)
FORCED VIBRATION ANALYSIS OF ROTATING CYCLIC STRUCTURES
BLADED DISC EXAMPLE 3 (CYC MODEL,FREQ+BASE ACCN LOAD,HARM I/O
KINDEX 15 SUBCASE 3

Figure 23

ORIGINAL PAGE IS
OF POOR QUALITY

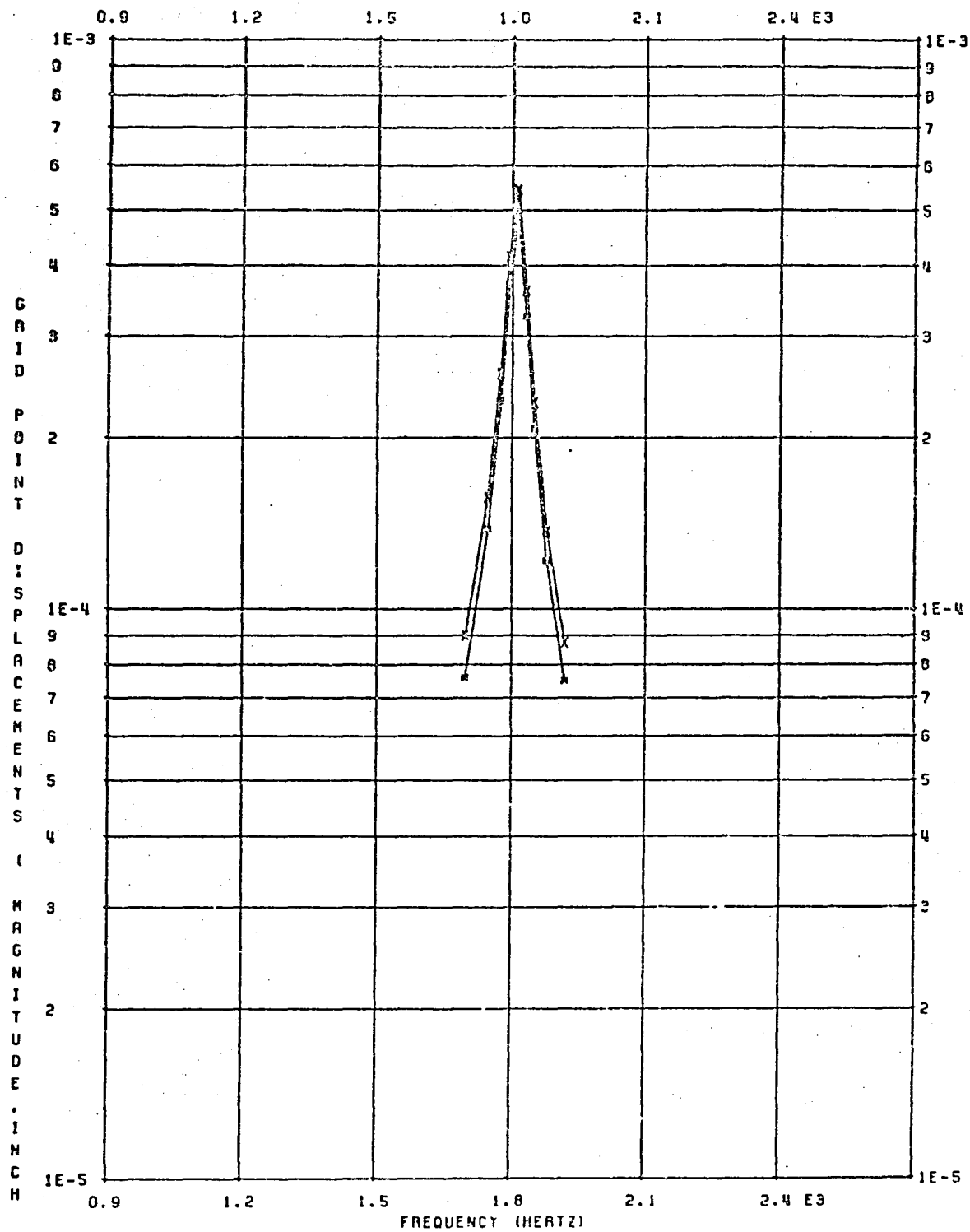

8(T3RM),18(T3RM)
FORCED VIBRATION ANALYSIS OF ROTATING CYCLIC STRUCTURES
BLADED DISC EXAMPLE 3 (CYC MODEL,FREQ+BASE ACCN LOAD,MARM I/O
KINDEX 2C SUBCASE 4

Figure 24

ORIGINAL PAGE IS
OF POOR QUALITY

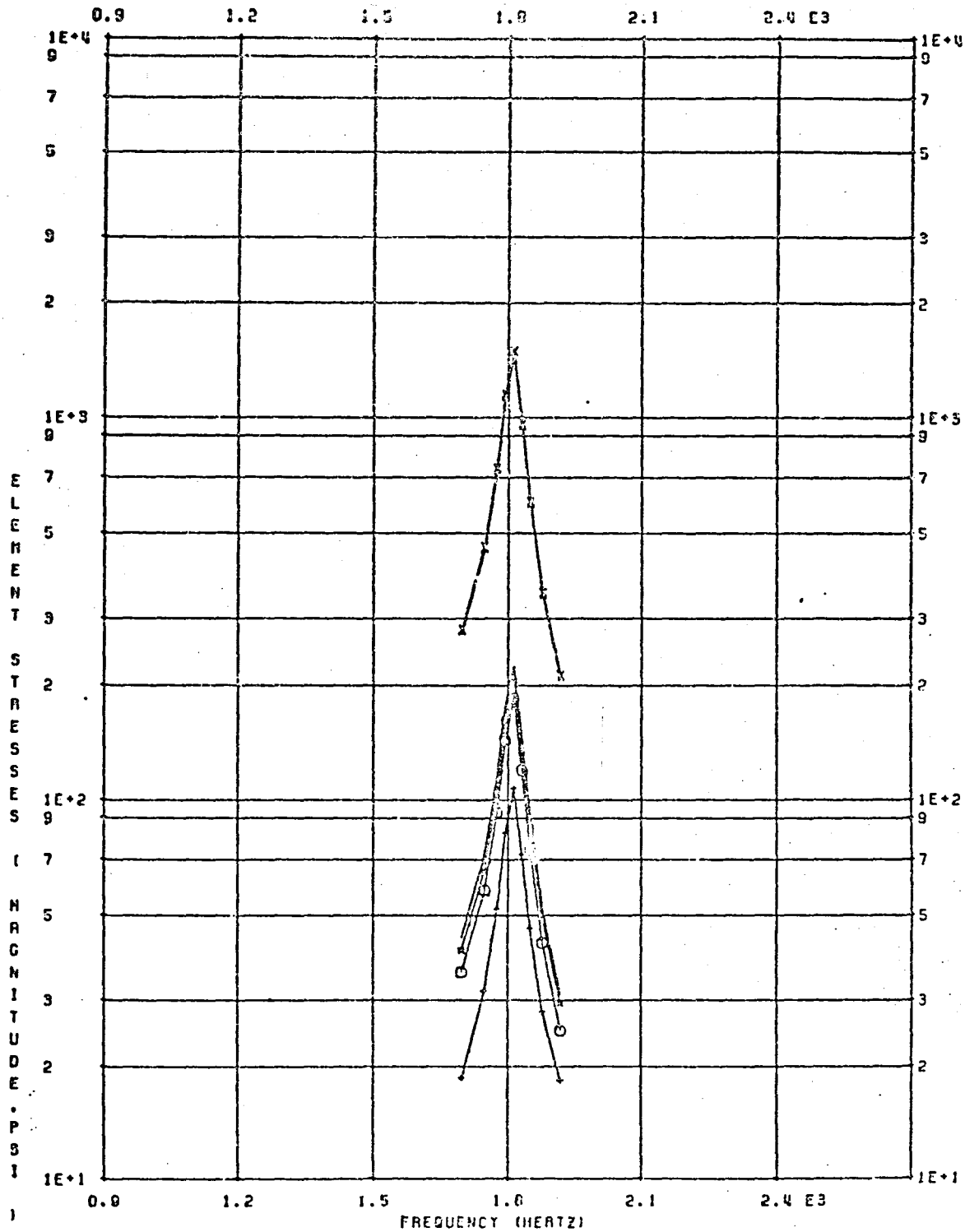

11(3),11(5),11(7),11(10),11(12),11(14)
FORCED VIBRATION ANALYSIS OF ROTATING CYCLIC STRUCTURES
BLADED DISC EXAMPLE 3 (CYC MODEL,FREQ+BASE ACCN LOAD,HARM I/O
KINDEX 2C SUBCASE 4

Figure 25

ORIGINAL PAGE IS
OF POOR QUALITY

TABLE 3: EFFECT OF CORIOLIS AND CENTRIPETAL ACCELERATIONS ON THE DISPLACEMENT RESPONSE OF GRID POINT 18 AT 600 RPS.

Frequency Hz	Example 2 Segment 1 (subcase 1) Mag. (in)/Phase (deg)	Example 3 k = 2c (subcase 4) Mag. (in)/Phase (deg)
1700	7.2655 E-5/349.4	7.6132 E-5/354.3
1750	1.3071 E-4/343.1	1.3844 E-4/347.3
1778	2.1580 E-4/332.7	2.3252 E-4/335.8
1796	3.4139 E-4/314.6	3.7252 E-4/315.2
1814	4.8374 E-4/269.9	4.9177 E-4/266.8
1832	3.4146 E-4/224.9	3.2655 E-4/225.5
1850	2.1451 E-4/206.6	2.0742 E-4/209.3
1880	1.2433 E-4/195.6	1.2214 E-4/199.2
1920	7.6125 E-5/190.4	7.5397 E-5/194.3

EXAMPLE 4

Description

This example uses the forced vibration capability with cyclic symmetry. The user input/output pertains to physical representation. Periodic loads are specified as functions of time on the segments of the bladed disc corresponding to k = 2. For clarity of illustration only, sinusoidal loads of varying amplitudes at a frequency of 1814 Hz are specified. The Fourier decomposition of these sine functions obviously contains contributions from first harmonic alone (ℓ = 1)-- the parameter LMAX accordingly has been set at 1 (ℓ = 0, 1c, 1s).

Input

1. Parameters:

   In addition to general input parameters,

   CYCIO = +1 physical cyclic input/output data
   KMIN = 2 minimum circumferential harmonic index
   KMAX = 2 maximum circumferential harmonic index
   LMAX = 1 maximum harmonic in the Fourier decomposition of periodic, time-dependent loads,
   NSEGS = 12 number of rotationally cyclic sectors
   RPS = 600.0 revolutions per second
   GKAD = FREQRESP } Specify the form in which the damping parameters are
   LGKAD = +1 } used.

2. Constraints:

   Same as general input constraints.

3. Loads:

$$P^n(t) = A(t) \cos\left(\overline{n-1} \cdot 2 \cdot \frac{2\pi}{12}\right) ,$$

   where n is the segment number,
   2 represents k = 2,
   12 represents the total number of segments in the bladed disc,
   $A(t) = A \cdot \sin(2\pi \cdot 1814 \cdot t)$.
   P is specified on TLOADi bulk data cards.

Results

Results are presented in Table 4 and are in good agreement with those from example 3.

TABLE 4: COMPARISON OF RESPONSE AT 1814 Hz.

Grid Pt.Disp. or Elem. Stresses	Example 3 k = 2c (subcase 4) Mag.(in)/Phase(deg)	Example 4 Segment 1 (subcase 1) Mag.(in)/Phase(deg)	Example 5 k = 2c (subcase 4) Mag.(in)/Phase(deg)
8 (T3RM), u_z	5.4297 E-4/82.6	5.4299 E-4/82.6	5.4299 E-4/82.6
18 (T3RM), u_z	4.9177 E-4/266.8	4.9180 E-4/266.8	4.9180 E-4/266.8
11 (3), $\sigma_{xx,1}$*	1.4841 E 3/84.7	1.4842 E 3/84.7	1.4842 E3/84.7
11 (5), $\sigma_{yy,1}$	2.0891 E 2/83.4	2.0892 E 2/83.4	2.0892 E2/83.4
11 (7), $\tau_{xy,1}$	1.0774 E 2/64.7	1.0775 E 2/64.7	1.0775 E2/64.7
11 (10), $\sigma_{xx,2}$*	1.4677 E 3/263.3	1.4678 E3/263.3	1.4678 E3/263.3
11 (12), $\sigma_{yy,2}$	2.2489 E 2/260.3	2.2491 E 2/260.4	2.2491 E2/260.4
11 (14), $\tau_{xy,2}$	1.8510 E 2/253.0	1.8511 E 2/253.0	1.8512 E2/253.0

* Fibre distances 1 and 2.

EXAMPLE 5

Description

This example uses the forced vibration capability with cyclic symmetry. The user input/output pertains to harmonic representation. Periodic loads are specified as functions of time for the circumferential harmonic index k = 2. For clarity of illustration only, sinusoidal loads are selected.

Input

1. Parameters:

   In addition to general input parameters,

   CYCIO = -1 harmonic cyclic input/output data
   KMIN = 2 minimum circumferential harmonic index
   KMAX = 2 maximum circumferential harmonic index
   LMAX = 1 maximum harmonic in the Fourier decomposition of periodic, time-dependent loads.
   NSEGS = 12 number of rotationally cyclic sectors
   RPS = 600.0 revolutions per second
   GKAD = FREQRESP } Specify the form in which the damping parameters
   LGKAD = +1 } are used.

2. Constraints:

   Same as general input constraints.

3. Loads:

$$\bar{P}^{2c}(t) = A \cdot \sin(2\pi \cdot 1814 \cdot t) ,$$

   specified on TLOADi bulk data cards.

Results

Results are presented in Table 4 and agree well with those from example 3.

5. CONCLUSIONS

1. A new capability has been developed and added to the general purpose finite element program NASTRAN Level 17.7 to conduct forced vibration analysis of tuned cyclic structures rotating about their axis of symmetry.

2. The effects of Coriolis and centripetal accelerations together with those due to the translational acceleration of the axis of rotation have been included.

3. A variety of user options is provided to specify the loads on the rotating structure.

4. Five interrelated examples are presented to illustrate the various features of this development.

6. RECOMMENDATIONS

1. This is a new capability and, therefore, the examples presented herein have been primarily designed to illustrate the various basic features of the development. Application to a variety of real problems would substantially contribute towards determining its merits and limitations with regards to its applicability, usefulness, and savings in modelling and computational time.

2. The capability should be extended to conduct forced response analysis using normal modes with cyclic symmetry as the basis.

3. Inclusion of induced and applied oscillatory aerodynamic loads within the capability would be a desirable step in solving the forced vibration problems of turbomachines.

ORIGINAL PAGE IS
OF POOR QUALITY

APPENDIX

INERTIAL LOADS DUE TO BASE ACCELERATION

The acceleration of the axis of rotation generates inertial loads at all grid points of the complete structure. In this appendix, the generation of these inertial loads and their transformation to frequency-dependent circumferential harmonic components are discussed.

As given by equation (27) of Section 2, the inertial forces on the three translational degrees of freedom at an arbitrary point P of the modelled cyclic sector, expressed in the global (displacement) coordinate system, are

$$\{P^G\} = -[M_2]\{\ddot{R}_0\} = [T^{BG}]\{P^B\} \quad , \tag{1}$$

where

$$\{P^B\} = \begin{Bmatrix} P_X \\ P_Y \\ P_Z \end{Bmatrix}^B = -\begin{bmatrix} m & 0 & 0 \\ 0 & m & 0 \\ 0 & 0 & m \end{bmatrix} \begin{bmatrix} 1 & 0 & 0 \\ 0 & c & s \\ 0 & -s & c \end{bmatrix} \begin{Bmatrix} \ddot{X}_0 \\ \ddot{Y}_0 \\ \ddot{Z}_0 \end{Bmatrix} \quad , \tag{2}$$

with $c \equiv \cos \Omega t$ and $s \equiv \sin \Omega t$.

Since all the cyclic sectors are identical in all respects except for the specified loads, no generality is lost in assuming, for simplicity, that the modelled sector is the n = 1 sector. Equation (1) can, then, be rewritten as

$$\{P^G\} = [T^{BG}] \begin{bmatrix} 1 & 0 & 0 \\ 0 & c_n & s_n \\ 0 & -s_n & c_n \end{bmatrix} \{P^B\} \quad , \tag{3}$$

where

$$\left.\begin{aligned} c_n &= \cos\left(\overline{n-1} \cdot 1 \cdot 2\pi/N\right), \quad \text{and} \\ s_n &= \sin\left(\overline{n-1} \cdot 1 \cdot 2\pi/N\right) \quad . \end{aligned}\right\} \tag{4}$$

Substituting equation (3) in equations (5) of Section 3, and noting that

$$\sum_{n=1}^{N} c_n \equiv 0 \tag{5}$$

$$
\left.
\begin{aligned}
&\sum_n s_n \equiv 0 \\
&\sum_n c_n \cdot \cos\left(\overline{n-1} \cdot k \cdot 2\pi/N\right) = N/2 \;, \quad k=1 \\
&\qquad\qquad\qquad\qquad\qquad\quad = 0 \;, \quad k\neq 1 \;, \\
&\sum_n s_n \cdot \cos\left(\overline{n-1} \cdot k \cdot 2\pi/N\right) \equiv 0 \;, \\
&\sum_n c_n \cdot \sin\left(\overline{n-1} \cdot k \cdot 2\pi/N\right) \equiv 0 \;, \\
&\sum_n s_n \cdot \sin\left(\overline{n-1} \cdot k \cdot 2\pi/N\right) = N/2 \;, \quad k=1 \\
&\qquad\qquad\qquad\qquad\qquad\quad = 0 \;, \quad k\neq 1 \;,
\end{aligned}
\right\} \qquad (5)\ \text{(contd)}
$$

the circumferential harmonic components of the base acceleration loads become

$$
\left.
\begin{aligned}
\{\overline{P}^{o}\}^{G} &= [T^{BG}] \begin{Bmatrix} P_X \\ 0 \\ 0 \end{Bmatrix}^{B} , \quad (\text{"k"} = 0) \\
\{\overline{P}^{1c}\}^{G} &= [T^{BG}] \begin{Bmatrix} 0 \\ P_y \\ P_z \end{Bmatrix}^{B} , \quad (\text{"k"} = 1c) \\
\{\overline{P}^{1s}\}^{G} &= [T^{BG}] \begin{Bmatrix} 0 \\ P_Z \\ -P_Y \end{Bmatrix}^{B} , \quad (\text{"k"} = 1s) \text{ , and} \\
\{\overline{P}^{kc,ks}\}^{G} &= \{0\} \text{ , all other "k".}
\end{aligned}
\right\} \qquad (6)
$$

In the present development, the components of base acceleration $\ddot{X}_0$, $\ddot{Y}_0$ and $\ddot{Z}_0$ are considered to be sinusoidal of frequency ω, and are specified as

$$
\left.
\begin{aligned}
\ddot{X}_0 &= \ddot{X}_{0,\,mag} \cos(\omega t + \phi_X) \;, \\
\ddot{Y}_0 &= \ddot{Y}_{0,\,mag} \cos(\omega t + \phi_Y) \;, \text{ and} \\
\ddot{Z}_0 &= \ddot{Z}_{0,\,mag} \cos(\omega t + \phi_Z) \;.
\end{aligned}
\right\} \qquad (7)
$$

From equation (2), therefore, we can write

$$\left.\begin{aligned} P_X^B &= -m\ddot{X}_{0,mag.} \cos(\omega t + \phi_X) \quad , \\ P_Y^B &= -m[\ddot{Y}_{0,mag} \cos \Omega t \cdot \cos(\omega t + \phi_Y) + \ddot{Z}_{0,mag} \sin \Omega t \cdot \cos(\omega t + \phi_Z)], \text{ and} \\ P_Z^B &= -m[-\ddot{Y}_{0,mag} \sin \Omega t \cdot \cos(\omega t + \phi_Y) + \ddot{Z}_{0,mag} \cos \Omega t \cdot \cos(\omega t + \phi_Z)]. \end{aligned}\right\} \quad (8)$$

The cosine and sine products in equations (8) can be expressed in terms of individual cosine and sine terms with frequencies $(\omega + \Omega)$ and $(\omega - \Omega)$.

The following conclusions about base acceleration loads can, therefore, be drawn by substituting equations (8) into equations (6):

1. The axial component of base acceleration, $\ddot{X}_0(\omega)$, contributes to $\overline{P}^0$ at excitation frequencies ω.

2. The lateral components of base acceleration, $\ddot{Y}_0(\omega)$ and $\ddot{Z}_0(\omega)$, contribute to $\overline{P}^{1c}$ and $\overline{P}^{1s}$ at excitation frequencies $(\omega \pm \Omega)$ for each ω specified.

SYMBOLS

B	Damping matrix
B_1	Coriolis acceleration coefficient matrix
D	Rayleigh's dissipation function
G	"Symmetric Components" transformation matrix
$\hat{I}, \hat{J}, \hat{K}$	Unit vectors along Inertial XYZ axes (Figure 3)
$\hat{I}_B, \hat{J}_B, \hat{K}_B$	Unit vectors along Basic X_B Y_B Z_B axes (Figure 3)
$\hat{i}, \hat{j}, \hat{k}$	Unit vectors along Global xyz axes (Figure 3)
K	Stiffness matrix
k	Circumferential harmonic index
ℓ	Time harmonic index
M	Mass matrix, number of time intervals per period (Figure 5)
M_1	Centripetal acceleration coefficient matrix
M_2	Base acceleration coefficient matrix
m	Mass
N	Number of cyclic sectors in the complete structure
P	Load vector
Q	Aerodynamic coefficient matrix
$\ddot{R}_0$	Base acceleration vector
$\vec{r}, \vec{R}, \vec{\rho}$	Position vectors (Figure 3)
T	Kinetic energy, coordinate system transformation matrix
t	Time
U	Strain energy
u	Physical displacement degrees of freedom
W	Virtual work
Ω	Rotational frequency
ω	Forcing frequency

SYMBOLS (Continued)

Superscripts

B	Basic
G	Global
K	Independent solution set in "symmetric components"
m	mth time instant
n	nth cyclic sector
-0	Fourier coefficients ("symmetric components")
-ℓc	
-ℓs	
-kc	
-ks	
-M/2	
-N/2	

REFERENCES

1. Smith, G. C. C., and Elchuri, V., "Aeroelastic and Dynamic Finite Element Analyses of a Bladed Shrouded Disk", NASA CR 159728, March 1980.

2. Elchuri, V., and Smith, G. C. C., "NASTRAN Level 16 Theoretical Manual Updates for Aeroelastic Analysis of Bladed Discs", NASA CR 159823, March 1980.

3. Elchuri, V., and Gallo, A. Michael, "NASTRAN Level 16 User's Manual Updates for Aeroelastic Analysis of Bladed Discs", NASA CR 159824, March 1980.

4. Gallo, A. Michael, and Dale, B. J., "NASTRAN Level 16 Programmer's Manual Updates for Aeroelastic Analysis of Bladed Discs", NASA CR 159825, March 1980.

5. Elchuri, V., and Gallo, A. Michael, "NASTRAN Level 16 Demonstration Manual Updates for Aeroelastic Analysis of Bladed Discs", NASA CR 159826, March 1980.

6. Gallo, A. Michael, Elchuri, V., and Skalski, S. C., "Bladed-Shrouded-Disc Aeroelastic Analyses: Computer Program Updates in NASTRAN Level 17.7", NASA CR 165428, December 1981.

7. NASTRAN Level 17.6 Theoretical Manual, NASA SP 221 (05), October 1980.

8. Elchuri, V., Gallo, A. Michael, and Skalski, S.C., "Forced Vibration Analysis of Rotating Cyclic Structures in NASTRAN", NASA CR 165429, December 1981.

End of Document